


December 2017

# The Electrochemical Deposition of Samarium and Europium Dissolved in Ionic Liquid Solvent

Bea Martinez

University of Nevada, Las Vegas, Bea.martinez2424@gmail.com

Follow this and additional works at: <https://digitalscholarship.unlv.edu/thesesdissertations>

 Part of the [Analytical Chemistry Commons](#), [Inorganic Chemistry Commons](#), and the [Physical Chemistry Commons](#)

---

## Repository Citation

Martinez, Bea, "The Electrochemical Deposition of Samarium and Europium Dissolved in Ionic Liquid Solvent" (2017). *UNLV Theses, Dissertations, Professional Papers, and Capstones*. 3150.

<https://digitalscholarship.unlv.edu/thesesdissertations/3150>

This Thesis is brought to you for free and open access by Digital Scholarship@UNLV. It has been accepted for inclusion in UNLV Theses, Dissertations, Professional Papers, and Capstones by an authorized administrator of Digital Scholarship@UNLV. For more information, please contact [digitalscholarship@unlv.edu](mailto:digitalscholarship@unlv.edu).

THE ELECTROCHEMICAL DEPOSITION OF SAMARIUM AND EUROPIUM  
DISSOLVED IN IONIC LIQUID SOLVENT

By

Eden Beatriz Martinez

Bachelor of Science—Biochemistry

University of Nevada, Las Vegas

2011

A thesis submitted in partial fulfillment  
of the requirements for the

Master of Science—Chemistry

Department of Chemistry and Biochemistry

College of Sciences

The Graduate College

University of Nevada, Las Vegas

December 2017



## **Thesis Approval**

The Graduate College  
The University of Nevada, Las Vegas

November 9, 2017

This thesis prepared by

Eden Beatriz Martinez

entitled

The Electrochemical Deposition of Samarium and Europium Dissolved in Ionic Liquid Solvent

is approved in partial fulfillment of the requirements for the degree of

Master of Science—Chemistry  
Department of Chemistry and Biochemistry

David Hatchett, Ph.D.  
*Examination Committee Chair*

Kathryn Hausbeck Korgan, Ph.D.  
*Graduate College Interim Dean*

Spencer Steinberg, Ph.D.  
*Examination Committee Member*

Dong Chan Lee, Ph.D.  
*Examination Committee Member*

Jacimaria Batista, Ph.D.  
*Graduate College Faculty Representative*

## Abstract

The Electrochemical Deposition of Samarium and Europium Dissolved in Ionic Liquid Solvent

By

Eden Beatriz Martinez

Dr. David Hatchett, Committee Chair

Professor of Chemistry

University of Nevada, Las Vegas

Rare-earth elements include the lanthanide series in the periodic table with the addition of scandium and yttrium. China produces approximately 95% of the world's rare-earths supply and is the largest consumer of the world's rare earth supply. Domestic production of rare-earth metals is a priority in the US. The domestic demand for rare-earth elements is largely based on their use in electronic devices, catalytic converters, and more importantly defense applications. Therefore, China's monopoly of rare-earth elements is viewed as a threat to national security. Although capital investments have resulted in an increase in domestic mining and refining of rare-earth materials, full scale production will take time. Alternatively, new methods for the reclamation of rare-earth materials could reduce the dependence on imported materials, as well as reduce electronic wastes in landfills. In this thesis, a path for the electrochemical reclamation of rare-earth materials is explored. Specifically, the dissolution of samarium carbonate and europium carbonate are examined in ionic liquid containing the acid N,N-bis(trifluoromethylsulfonyl)imide, HTf<sub>2</sub>N. The use of carbonate derivatives facilitates the dissolution of the rare-earth species through the formation of carbonic acid. The carbonic acid can then be purged through a decomposition reaction that produces carbon dioxide and water. The dissolution and coordination of the lanthanide with

bis(trifluoromethylsulfonyl)imide anion,  $\text{Tf}_2\text{N}$ , is evaluated using a spectroscopic method (UV-Vis). The electrochemistry of samarium and europium is examined in the ionic liquid and the studies demonstrate that electrochemical deposition of samarium and europium species occur. SEM/EDX analysis of the deposit on a graphite electrode confirms the electrochemical reclamation of samarium and europium metal.

## Acknowledgements

I would like to start by thanking Dr. David Hatchett. It is an honor to have been your graduate student and I strive to continue the work ethics that you have bestowed upon me. I could not have been blessed with a more understanding and very supportive advisor. Thank you for your guidance and help throughout this whole master's project, as well as your patience until the very end. Please give me the recipe for your dulce de leche.

I would also like to acknowledge my committee members: Dr. Spencer Steinberg, Dr. Dong Chan Lee, and Dr. Jacimaria Batista. Dr. Spencer Steinberg, your dry humor and daily dose of sarcasm is always appreciated. Dr. Dong Chan Lee, your enthusiasm for organic chemistry may not be shared by more than half the population, but you never gave up on trying to spread your passion for organic chemistry. Dr. Jacimaria Batista, thank you for providing additional context and an environmental perspective on my research that I hadn't thought of before.

I would like to thank my research lab mates: Janelle Droessler, Nicole Goodwin, Morgan Jarvis, Katherine Thornock, Cassara Higgins, and our newly initiated member Phillip Hammer. I will always be grateful for the friendship and company that you have provided me during the darkest times. All the data analysis and long lab days have allowed for friendships that I hope to keep for life. A special thank you goes to the other graduate students who have helped me along the way: Jarod Wolffis, Nicole Millick, Natiera Magnuson, Amit Sharma, and Derek McLain. More thank you goes to Jung Jae Koh, the lab coordinator, for the organic chemistry knowledge and techniques that I now use daily for work.

I don't think for a minute that I would have survived the Department of Chemistry and Biochemistry without the help of Mark Miyamoto, Deborah Masters, Bianca Rideout, and Carolyn

Hatchett. Thank you for all your help. I now truly believe that not all heroes wear capes. To Keala “Ala” Kiko, I will always be in your debt for your reminder emails, as well as your help throughout every process of the Graduate College. Dr. Kathleen Robins, thank you for the guidance as the Graduate Coordinator for the Department of Chemistry and Biochemistry.

My deepest gratitude goes to my family and friends. There clearly are no words that would even begin to say how grateful I am for all your love and support. To my mom and dad: thank you for the financial support, so that I never have to be homeless or go hungry. My brother and sister: thank you for believing in me and always telling me to never give up. To my friends: thank you for never holding a grudge when I’d disappear during graduate school years and for never stopping to check in to see if I still exist.

My thesis would not have been possible without each and every one of you.

## Table of Contents

Abstract.....	iii
Acknowledgements.....	v
List of Tables .....	ix
List of Figures .....	x
List of Equations .....	xii
Chapter 1. Introduction .....	1
1.1    Ionic Liquid.....	1
1.2    Electrochemistry in IL .....	3
1.2.1    Electrochemistry of metals dissolved in IL .....	5
1.2.2    Electrochemistry of f-elements .....	8
1.3    Metal dissolution.....	10
1.3.1    f-element metal dissolution.....	12
1.4    Optical spectroscopy of f-elements in ILs .....	13
1.5    Motivation.....	14
1.6    Present studies (hypothesis).....	16
Chapter 2. Experimental Methods .....	17
2.1    Dissolution methods: Comparison of previous methods with direct dissolution ...	17
2.2    Materials .....	18
2.2.1    Samarium Dissolution .....	18
2.2.2    Europium Dissolution .....	19
2.3    Acid neutralization and water removal .....	20
2.4    Spectroscopy .....	21
2.5    Electrochemistry .....	22
2.5.1    Cyclic Voltammetry.....	22
2.5.2    Amperometric Deposition.....	25
2.6    SEM/EDX.....	26
Chapter 3. Samarium and Europium Dissolution and Electrochemistry .....	27
3.1    Introduction.....	27
3.2    Samarium and Europium Dissolution.....	28
3.2.1    UV-Vis Spectroscopy Results.....	28
3.3    Electrochemistry .....	32



3.3.1	Cyclic Voltammetry.....	32
3.3.2	Samarium and Europium Deposition on Grafoil .....	40
3.4	SEM/EDX.....	42
3.4.1	SEM/EDX of the electrodeposition .....	42
3.5	Conclusion.....	50
Chapter 4.	Conclusion.....	51
References	.....	52
Curriculum Vitae	.....	55

## List of Tables

<b>Table 1.</b> Potential windows of various ionic liquids. <sup>10</sup> *[EtMeImCl]/AlCl <sub>3</sub> /NaCl is a first generation IL.....	4
<b>Table 2.</b> Potential windows (V) for dry IL and with water. <sup>9</sup> .....	4

## List of Figures

<b>Figure 1.</b> Potential window for an aqueous system spans between 1.23 to 0 V. Potential for lanthanide metal deposition at more negative potential between -2 to -3 V.....	6
<b>Figure 2.</b> Cyclic voltammetry of dry [Me <sub>3</sub> N <sup>n</sup> Bu][Tf <sub>2</sub> N] between 0 V to -3.1 V with no visible hydrogen evolution or water oxidation. ....	6
<b>Figure 3.</b> Lanthanide dissolution: Lanthanide carbonate→IL addition→H <sub>2</sub> O addition→shaken mixture→after the addition of HTf <sub>2</sub> N .....	20
<b>Figure 4.</b> pH of aqueous layer started at 1, but became less acidic as the process was repeated. ....	21
<b>Figure 5.</b> Cyclic voltammetry of 5 mM ferrocene in [Me <sub>3</sub> N <sup>n</sup> Bu][Tf <sub>2</sub> N]. ....	24
<b>Figure 6.</b> Flow diagram for the dissolution and recovery of lanthanide metals.....	27
<b>Figure 7.</b> UV-Vis absorbance spectra IL, [Me <sub>3</sub> N <sup>n</sup> Bu][Tf <sub>2</sub> N], and IL containing 150 mM Sm. ....	29
<b>Figure 8.</b> UV-Vis absorbance spectra IL, [Me <sub>3</sub> N <sup>n</sup> Bu][Tf <sub>2</sub> N], and IL containing 150 mM Eu. ....	30
<b>Figure 9.</b> Top: IL purged with dry N <sub>2</sub> gas for 4, 6, and 12 hours. Middle: Pristine IL out of the bottle. Bottom: IL saturated with H <sub>2</sub> O. <sup>49</sup> .....	33
<b>Figure 10.</b> From top to bottom: Cyclic voltammetric responses on Au disc electrode of Dried IL, IL saturated with H <sub>2</sub> O, IL saturated with H <sub>2</sub> O and 0.5 M HTf <sub>2</sub> N, and IL after H <sub>2</sub> O removal and HTf <sub>2</sub> N neutralization (as well as an enlarged version of the reduction scan).....	34
<b>Figure 11.</b> Cyclic voltammetry of the background IL (grey) and 150 mM samarium dissolved in IL (first cycle). ....	37
<b>Figure 12.</b> Cyclic voltammetry of the background IL (grey) and 150 mM samarium dissolved in IL (20 cycles). ....	38
<b>Figure 13.</b> Cyclic voltammetry of the background IL (grey) and 150 mM europium dissolved in IL (first cycle). ....	39
<b>Figure 14.</b> Cyclic voltammetry of the background IL (grey) and 150 mM europium dissolved in IL (20 cycles). ....	40
<b>Figure 15.</b> Amperometric deposition of 150 mM samarium in IL with HTf <sub>2</sub> N held at -2.6 V for 24 hours. ....	41
<b>Figure 16.</b> Amperometric deposition of 150 mM europium in IL with HTf <sub>2</sub> N held at -2.4 V for 24 hours. ....	42
<b>Figure 17.</b> Grafoil 100x under SEM used for background IL.....	43
<b>Figure 18.</b> Grafoil 2000x under SEM used for background IL.....	44
<b>Figure 19.</b> Grafoil 2000x EDX after exposure to IL without washing. ....	44
<b>Figure 20.</b> SEM of Samarium deposits at 100x magnification. ....	45
<b>Figure 21.</b> SEM of Samarium deposits at 2000x magnification. ....	46
<b>Figure 22.</b> Samarium metal 2000x EDX.....	46

<b>Figure 23.</b> SEM of Europium deposits at 100x magnification. ....	48
<b>Figure 24.</b> SEM of Europium deposits at 2000x magnification. ....	49
<b>Figure 25.</b> Europium metal 2000x EDX. ....	49

## List of Equations

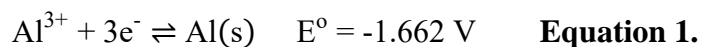
<b>Equation 1</b>	$\text{Al}^{3+} + 3\text{e}^- \rightleftharpoons \text{Al(s)} \quad E^\circ = -1.662 \text{ V}$	1
<b>Equation 2</b>	$\text{O}_2 + 2\text{H}_2\text{O} + 4\text{e}^- \rightleftharpoons 4\text{OH}^- \quad E^\circ = 0.401 \text{ V}$	3
<b>Equation 3</b>	$\text{O}_2 + 4\text{H}^+ + 4\text{e}^- \rightleftharpoons 2\text{H}_2\text{O} \quad E^\circ = 1.229 \text{ V}$	3
<b>Equation 4</b>	$2\text{H}^+ + 2\text{e}^- \rightleftharpoons \text{H}_2 \quad E^\circ = 0.0000 \text{ V}$	4
<b>Equation 5</b>	$A = -\log I/I_0 = -\log T$	22
<b>Equation 6</b>	$A = -\log T = \epsilon bc$	22
<b>Equation 7</b>	$\text{Sm}_2(\text{CO}_3)_3 + 6(\text{CF}_3\text{SO}_2)_2\text{NH} \rightarrow 3\text{H}_2\text{CO}_3 + 2\text{Sm}^{3+} + 6(\text{CF}_3\text{SO}_2)_2\text{N}^-$	28
<b>Equation 8</b>	$\text{Eu}_2(\text{CO}_3)_3 + 6(\text{CF}_3\text{SO}_2)_2\text{NH} \rightarrow 3\text{H}_2\text{CO}_3 + 2\text{Eu}^{3+} + 6(\text{CF}_3\text{SO}_2)_2\text{N}^-$	28
<b>Equation 9</b>	$\text{Sm}^{3+} + \text{e}^- \rightleftharpoons \text{Sm}^{2+} \quad E^\circ = -1.749 \text{ V}$	32
<b>Equation 10</b>	$\text{Sm}^{3+} + 3\text{e}^- \rightleftharpoons \text{Sm} \quad E^\circ = -2.503 \text{ V}$	32
<b>Equation 11</b>	$\text{Sm}^{2+} + 2\text{e}^- \rightleftharpoons \text{Sm} \quad E^\circ = -2.879 \text{ V}$	32
<b>Equation 12</b>	$\text{Eu}^{3+} + \text{e}^- \rightleftharpoons \text{Eu}^{2+} \quad E^\circ = -0.559 \text{ V}$	32
<b>Equation 13</b>	$\text{Eu}^{3+} + 3\text{e}^- \rightleftharpoons \text{Eu} \quad E^\circ = -2.190 \text{ V}$	32
<b>Equation 14</b>	$\text{Eu}^{2+} + 2\text{e}^- \rightleftharpoons \text{Eu} \quad E^\circ = -3.011 \text{ V}$	32

## Chapter 1. Introduction

### 1.1 Ionic Liquid

Ionic liquids (IL) were first reported in 1914 by Paul Walden based on his work with ethylammonium nitrate.<sup>1</sup> The very first IL was formed by heating an organic ethylamine with concentrated nitric acid giving the following ethylammonium cation,  $\text{EtNH}_3^+$ , and nitrate anion,  $\text{NO}_3^-$ .<sup>1</sup> ILs can be defined as solutions that are comprised of a cation and anion pair that are liquid below  $100^\circ\text{C}$ .<sup>2</sup> The IL remains a liquid at room temperature based on the minimization of cation/anion interactions which reduces the attraction and destabilizes crystal formation.<sup>3</sup> Traditionally, ILs are comprised of a bulky organic cation, such as N-alkylpyridinium or N, N'-dialkylimidazolium, combined with an inorganic anion, such as  $\text{BF}_4^-$ ,  $\text{Cl}^-$ ,  $\text{I}^-$ ,  $\text{CF}_3\text{SO}_3^-$ , and  $\text{AlCl}_4^-$ .<sup>4</sup> The product of the organic reaction between the organic cation and inorganic anion produces at least one ion with delocalized charge which prevents the formation of a stable crystal lattice structure.<sup>2</sup> The resulting ionic liquid solution has physical and chemical properties that are similar to inorganic salts.<sup>5</sup>

The physical and chemical properties of ionic liquid systems make them attractive solvents for the deposition of electropositive metals. For example, electrochemical deposition of aluminum metal has been demonstrated with first generation ILs comprised of quaternary ammonium salts with halide anions.<sup>6</sup> Therefore, the advantage of using these ILs is that they have potential windows greater than 3 V that extend to sufficiently negative values to facilitate the deposition of metal species that cannot be achieved from aqueous solutions.<sup>7</sup>



However, there are some drawbacks to first generation ILs. They often required elevated temperatures  $\geq 40^{\circ}\text{C}$  to achieve metal deposition.<sup>6</sup> Elevated temperatures enhance metal deposition by reducing viscosity which increases the overall conductivity of the solution.<sup>6</sup> First generation ILs are sensitive to water and impurities which cause degradation.<sup>6</sup> Therefore, the ILs had to be kept under a stream of dry, inert gas to minimize water uptake and oxidation which would cause severe deterioration of the IL over time.<sup>6</sup> The stability issue associated with first generation IL make them extremely difficult to use under ambient conditions.<sup>7</sup>

The degradation of ILs under atmospheric conditions was addressed in the 1990s with ILs that were more stable in the presence of water and secondary contaminants. Second generation ILs utilize hydrophobic anions, such as tri-fluoromethanesulfonate ( $\text{CF}_3\text{SO}_3^-$ ), bis(trifluoromethanesulfonyl)imide ( $((\text{CF}_3\text{SO}_2)_2\text{N}^-)$ , tris(trifluoromethanesulfonyl)methide ( $((\text{CF}_3\text{SO}_2)_3\text{C}^-)$ , tetrafluoroborate ( $\text{BF}_4^-$ ), and hexafluorophosphate ( $\text{PF}_6^-$ ), based on their low reactivity with water.<sup>4</sup> In addition, these ILs can also be easily dried to below 1ppm of water under vacuum between  $100\text{-}150^{\circ}\text{C}$  to minimize the influence of water on the physical properties.<sup>4</sup> The ILs have been alluded to as “green” solvents because they can be recycled with little or no use of volatile organic compounds.<sup>2</sup> In addition, the low volatility of ILs ensures that most products can be distilled, or extracted with water or hydrocarbon solvents.<sup>2</sup> ILs are hydrophobic, making them less likely to react with water and less likely to produce acidic species through hydrolysis.<sup>6, 8</sup> ILs are also an ideal solvent for electrochemical systems due to its low vapor pressure in comparison to volatile organic compounds.<sup>2, 4</sup> ILs have a wide potential window and high ionic conductivity, making them ideal for use as electrolytes in photovoltaics, fuel cells, batteries, and electrochemical sensors.<sup>2, 4</sup>

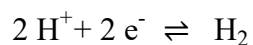
## 1.2 Electrochemistry in IL

The properties of different cation/anion pairs produce different physical characteristics. For this reason, ILs have been called “designer solvents” where the cation and anion are used to adjust the solvent properties for specific applications.<sup>9</sup> We are primarily concerned with the role the cation/anion pair play in the electrochemical limits for oxidation/reduction which define the potential window. For ILs, the electrochemical potential window is determined by the potentials associated with the oxidation of the anion and the reduction of the cation used to make the IL. Based on these limitations the potential windows have been measured for a variety of ILs with some exceeding 6 V.<sup>2</sup> **Table 1** provides example of ILs with their cathodic and anodic limits with the overall potential window.

Water is considered to be an impurity in IL for electrochemistry. Atmospheric water can be absorbed by hydrophobic ILs directly impacting physical parameters including the viscosity, conductivity, and potential window. For example, increasing water content in the IL reduces viscosity.<sup>9</sup> The viscosity directly impacts the conductivity of IL, which enhances the mass transport of the analyte and thus increases conductivity.<sup>9</sup> Although an increase in conductivity is ideal in terms of the electrochemical mass transport, narrowing of the potential window can limit the species that can be examined in the IL.<sup>9</sup> Water dissociation within the IL directly influences the potential window through the formation of protons. The reduction in potential window is based on side reaction during the cathodic and anodic scan due to hydrogen evolution and water oxidation reactions.<sup>9</sup> When there is water present in the IL, the positive and negative potential limits are bounded by water oxidation and hydrogen evolution, respectively.







$$E^\circ = 0.0000 \text{ V} \quad \text{Equation 4.}$$

Ionic liquids	Cathodic limit (V)	Anodic limit (V)	Potential window		
[EtMeIm] <sup>+</sup> [F] <sup>-</sup>	0.7	2.4	3.1	Me	methyl
[EtMeIm] <sup>+</sup> [BF <sub>4</sub> ] <sup>-</sup>	-2.1	2.2	4.3	Et	ethyl
[EtMeIm] <sup>+</sup> [N(CF <sub>3</sub> SO <sub>2</sub> ) <sub>2</sub> ] <sup>-</sup>	-1.8	2.5	4.3	Bu	butyl
[EtMeIm] <sup>+</sup> [(CN) <sub>2</sub> N] <sup>-</sup>	-1.6	1.4	3.0	Pr	Propyl
[BuMeIm] <sup>+</sup> [BF <sub>4</sub> ] <sup>-</sup>	-1.6	4.5	6.1	Im	Imidazolium
[BuMeIm] <sup>+</sup> [PF <sub>6</sub> ] <sup>-</sup>	-1.1	2.1	3.2	Py	Pyrrolidinium
[nPrMePy] <sup>+</sup> [N(CF <sub>3</sub> SO <sub>2</sub> ) <sub>2</sub> ] <sup>-</sup>	-2.5	2.8	5.3	N	Ammonium
[nBuMePy] <sup>+</sup> [N(CF <sub>3</sub> SO <sub>2</sub> ) <sub>2</sub> ] <sup>-</sup>	-3.0	3.0	6.0	Pp	Piperidinium
[nMe <sub>3</sub> BuN] <sup>+</sup> [N(CF <sub>3</sub> SO <sub>2</sub> ) <sub>2</sub> ] <sup>-</sup>	-2.0	2.0	4.0	P	Pyridinium
[nPrMe <sub>3</sub> N] <sup>+</sup> [N(CF <sub>3</sub> SO <sub>2</sub> ) <sub>2</sub> ] <sup>-</sup>	-3.2	2.5	5.7		
[BuP] <sup>+</sup> [BF <sub>4</sub> ] <sup>-</sup>	-1.0	2.4	3.4		
[MePrPp] <sup>+</sup> [N(CF <sub>3</sub> SO <sub>2</sub> ) <sub>2</sub> ] <sup>-</sup>	-3.3	2.3	5.6		
[EtMeImCl]/AlCl <sub>3</sub> /NaCl*	-2.2	2.3	4.5		

**Table 1.** Potential windows of various ionic liquids.<sup>10</sup> \*[EtMeImCl]/AlCl<sub>3</sub>/NaCl is a first generation IL.

Ionic liquids	vacuum-dried	atmospheric	wet
[P <sub>14,6,6,6</sub> ][Tf <sub>2</sub> N]	5.2	3.2	1.8
[C <sub>4</sub> mppyrr][Tf <sub>2</sub> N]	4.2	3.0	2.0
[C <sub>6</sub> mim][FAP]	4.6	3.0	2.5
[C <sub>4</sub> mim][Tf <sub>2</sub> N]	4.3	2.9	2.8
[C <sub>4</sub> dmim][Tf <sub>2</sub> N]	4.7	3.3	2.9
[N <sub>6,2,2,2</sub> ][Tf <sub>2</sub> N]	4.7	2.3	2.2
[C <sub>4</sub> mim][PF <sub>6</sub> ]	4.8	3.9	2.6
[C <sub>2</sub> mim][Tf <sub>2</sub> N]	4.2	2.8	2.6
[C <sub>4</sub> mim][BF <sub>4</sub> ]	4.6	2.4	2.0
[C <sub>4</sub> mim][I]	2.0	1.9	1.6
[C <sub>4</sub> mim][OTf]	4.2	3.3	2.7
[C <sub>6</sub> mim][Cl]	3.0	2.9	2.4

**Table 2.** Potential windows (V) for dry IL and with water.<sup>9</sup>

In addition, both the cation and anion influence the physical properties of the IL based on the hydrophobicity, hydrophilicity and miscibility with water.<sup>9</sup> Increases in the alkyl chain length of cation substituents will influence the hydrophobicity of the IL and the phase separation with water.<sup>9</sup> In contrast, the anion of the IL is the main factor in hydrophilicity and directly influences water uptake by the IL and the extent it can be dried.<sup>9</sup> Therefore, most ILs are hygroscopic, including those that are considered to be hydrophobic, and they absorb water from the atmosphere.<sup>11</sup> These water molecules tend to bind to the anion via H-bonding which indicates they can be removed from the IL solution by simply purging with desiccated inert gas or by heating.<sup>11</sup> Although removing all of the water from the IL is impossible<sup>12</sup>, it can be minimized. Furthermore, there are cases where the miscible water within the IL can be exploited in the dissolution of materials that are not typically soluble in IL.<sup>11</sup>

ILs have been considered and extensively studied for their stability as a solution. Materials that could not be deposited in aqueous baths, such as semiconductors or metals that are typically sensitive to water, can be directly electroplated when using IL as a media.<sup>2</sup> Some metal deposition occur at a more negative potential than an aqueous media will allow. Therefore, some metal deposition cannot be done in an aqueous media due to its side reactions, such as electrolysis of water.

### 1.2.1 Electrochemistry of metals dissolved in IL

The potential windows of ILs encompass the reduction potentials to convert all known elements from their oxidized to fully reduced forms. Theoretically, oxidized forms of alkali earth, lanthanide, actinide, and transition metals can be recovered as metals from ILs. Electrochemical deposition of metal species that are sensitive to hydrolysis can be achieved from purged ILs. Side

reactions, such as hydrogen evolution and water oxidation, do not contribute to the overall electrochemical reactions of the metal species in dried IL.

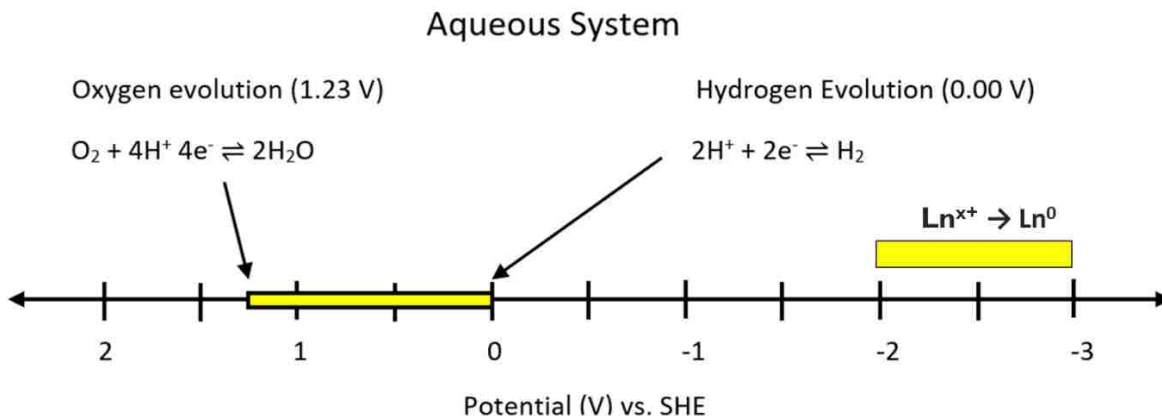


**Figure 1.** Potential window for an aqueous system spans between 1.23 to 0 V. Potential for lanthanide metal deposition at more negative potential between -2 to -3 V.

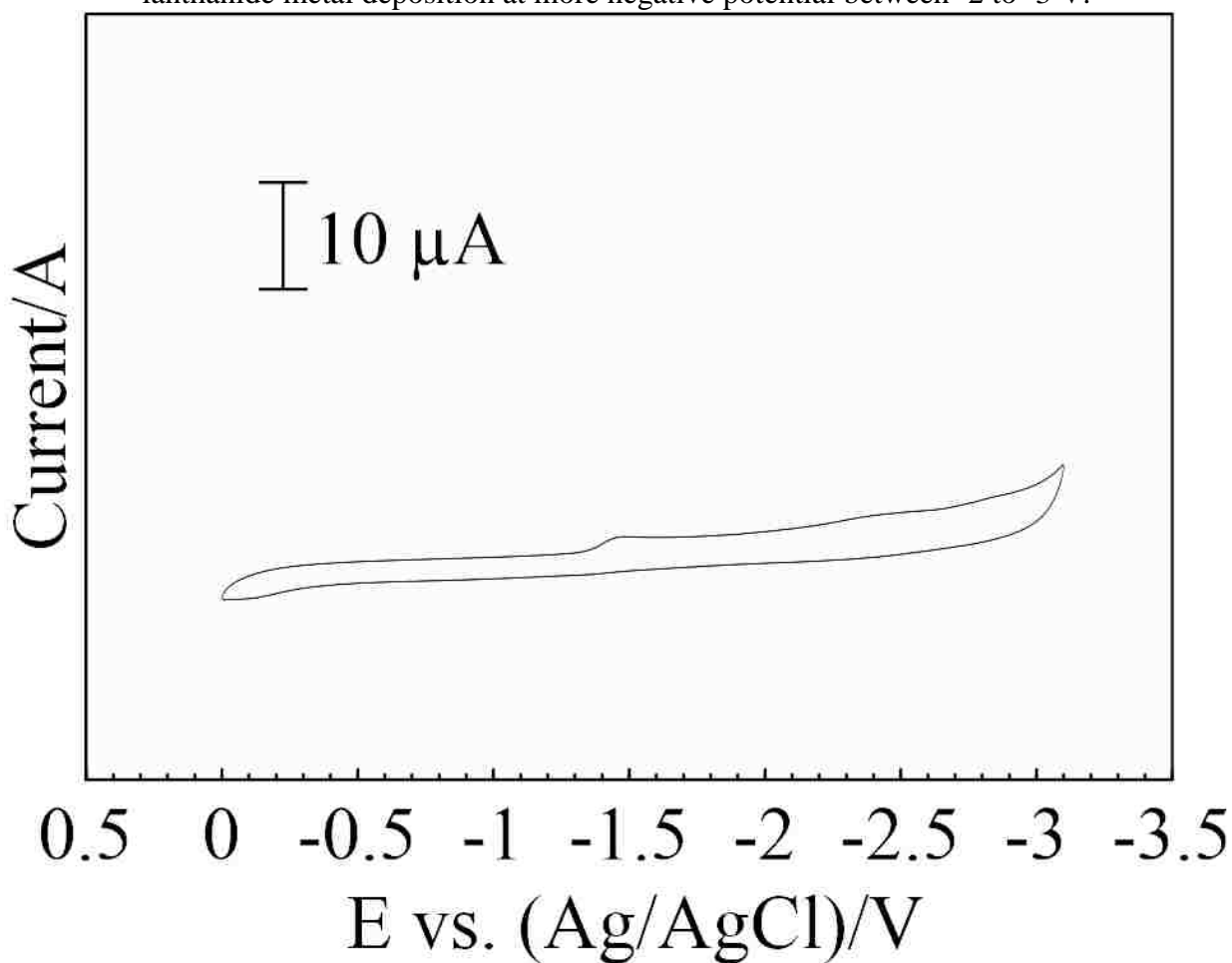


**Figure 2.** Cyclic voltammetry of dry  $[\text{Me}_3\text{N}^n\text{Bu}][\text{Tf}_2\text{N}]$  between 0 V to -3.1 V with no visible hydrogen evolution or water oxidation.

A few examples are provided to show the versatility of the IL system in the deposition of chemical species. The deposition of aluminum metal can be achieved in ILs. The reduction of  $\text{Al}^{3+}$  to metal occurs at -1.662 V vs. NHE in an aqueous solution based on the formation of an amalgam with Hg. The deposition can be achieved on steel to prevent corrosion using IL solutions. If stainless steel were utilized for the deposition of Al metal in an aqueous alkaline solution, hydrogen evolution would occur at -0.8277 V vs NHE.<sup>13</sup> The reduction of  $\text{Al}^{3+}$  would be eliminated and hydrogen evolution would dominate. In addition, sufficient positive potentials can be attained using ILs such that the dissolution of aluminum can be achieved. However, the cation of the IL can influence the dissolution and deposition of the Al producing different grain sizes associated with the deposits.<sup>2</sup> The morphology change for the deposits is likely related to the cation solvation layers that formed at the interface between the electrode and the IL at negative potentials.<sup>2</sup>

The negative potential limit of most ILs suggests that the metal deposition from mixed solutions is also possible. Thus, deposition of binary and higher order alloys is possible based on the potential window of most ILs. Moreover, the oxidation/reduction of variable oxidation states of transition metals can be achieved. In some cases, the formation of multi-valent species inhibits the electrochemical deposition.<sup>2</sup> For example, the deposition of titanium from titanium chloride can be achieved, but the method used requires heating between 170 °C - 200 °C and creates  $\text{SO}_2$  gas as a byproduct.<sup>14</sup> In some cases, the process is inhibited due to the formation of titanium halides such as  $\text{TiCl}_4^{2-}$  and  $\text{TiCl}_6^{2-}$ .<sup>15</sup> These species are linked through the reduction process and both remain soluble in the IL. In addition, the deposition of Ti can typically be achieved through the formation of alloys with other metals, such as an aluminum-molybdenum-titanium.<sup>2</sup> No elemental titanium deposition from titanium halides has been achieved through

electrodeposition.<sup>15</sup> Rather, titanium oxide deposits are achieved with degradation of the IL contributing the necessary oxygen.

Other studies of metal dissolution in ILs have been investigated with various electrodes. The study by Aldous, et al. illustrates gold deposition on Pt, Au, and GC electrodes, but the  $[\text{HCl}_2]^-$  in solution dominates the anodic scans.<sup>16</sup> Their studies also show that deposition is hindered by water and when the anion of the IL is changed.<sup>16</sup>

Finally, the deposition of non-metal species can also be achieved using IL solutions. For example, the deposition of semiconductor species Si and Ge have been achieved using IL solutions. Photoluminescent  $\text{Si}_x\text{Ge}_{1-x}$  has been electrodeposited from an ultrapure IL containing silicon and germanium halides.<sup>17</sup> The purity of the  $\text{Si}_x\text{Ge}_{1-x}$  were sufficient that photoluminescence and visible color changes could be observed for the binary species during deposition.<sup>17</sup> The studies suggest that ILs can be utilized for the deposition of semiconductor materials to reduce manufacturing costs for solar cells.<sup>17</sup>

### 1.2.2 Electrochemistry of f-elements

The negative potential limit of most ILs encompasses the standard reduction potentials of most f-elements. In some cases, the reduction of the cation occurs prior to the deposition of the f-element. Water can also influence the reaction of actinides species through hydrolysis reactions to form oxides which hinders metal deposition.<sup>18</sup> In the presence of water hydrogen evolution will dominate the electrochemical process eliminating the formation of either lanthanide or actinide metals at the electrochemical interface. The electrodeposition of lanthanides and actinides are achieved using anhydrous molten salt baths.<sup>18</sup> In addition, ILs without water represent a viable solvent system for the electrochemical recovery of f-elements without the required energy input of molten salts.<sup>18</sup>

The ability to recover f-element is also strongly dependent on the reduction potential of the cation in the IL. If the cation is reduced before the f-element, significant degradation of the IL can occur which hinders material recovery.<sup>18</sup> For example, the reduction of the imidazolium cation results in decomposition based on the ring opening, which changes the properties of the IL.<sup>18</sup> In contrast, quaternary ammonium salts have better cathodic stability, but suffer from high viscosity which minimizes diffusion limited electrochemistry processes.<sup>18</sup> Fortunately, the viscosity can be adjusted using different chemical species such as  $[\text{Tf}_2\text{N}]^-$  (bis(trifluoromethylsulfonyl)imide or  $((\text{CF}_3\text{SO}_2)_2\text{N})^-$ ) when the alkyl chains of the cation consists of six carbons or less.<sup>18</sup> The electrochemical window can span from 3 V to 6 V, depending on the electrode used.<sup>2, 7, 19</sup>

Studies of lanthanide depositions from  $\text{AlCl}_3$ - $[\text{C}_2\text{mim}]\text{Cl}$  saturated with  $\text{LaCl}_3$  showed individual aluminum metal deposits with some aluminum-lanthanum alloy.<sup>18</sup> However, the alloy was deficient in lanthanum at 0.12% in comparison to aluminum.<sup>18</sup> In contrast, an alloy containing cobalt, zinc, and dysprosium has been obtained with up to 24.5 wt % dysprosium using  $\text{ZnCl}_2$ - $[\text{C}_2\text{mim}]\text{Cl}$  IL with dissolved  $\text{CoCl}_2$  and  $\text{DyCl}_3$ .<sup>18</sup> While no isolated dysprosium metal was identified it is likely the species is incorporated as the divalent cation is in the alloy.<sup>18</sup>

For comparison, the thorium (IV) compound,  $\text{Th}(\text{Tf}_2\text{N})_4(\text{HTf}_2\text{N}) \cdot 2\text{H}_2\text{O}$  was synthesized and is dissolved into  $[\text{Me}_3\text{N}^n\text{Bu}][\text{Tf}_2\text{N}]$  to obtain a solution high in Th.<sup>20</sup> The target deposit was Th metal. However, the hydrated crystal is electrodeposited to form  $\text{ThO}_2$  on the electrode surface due to the complexed water.<sup>20</sup> The data suggests that the deposition of lanthanide or actinide metals may be minimized if the metal species dissolved in IL is hydrated. For example, lanthanide hydrated complexes such as  $\text{Ln}(\text{Tf}_2\text{N})_3(\text{HTf}_2\text{N}) \cdot 3\text{H}_2\text{O}$ ,  $\text{Eu}(\text{Tf}_2\text{N})_3(\text{HTf}_2\text{N}) \cdot 3\text{H}_2\text{O}$ , and  $\text{Sm}(\text{Tf}_2\text{N})_3(\text{HTf}_2\text{N}) \cdot 3\text{H}_2\text{O}$  were also dissolved in the chosen IL,  $[\text{Me}_3\text{N}^n\text{Bu}][\text{Tf}_2\text{N}]$ , due to the weakly coordinated  $\text{Tf}_2\text{N}$  ligand.<sup>21</sup> However, only the lanthanide oxide species were obtained from

the electrochemical deposition of the hydrated complexes. Finally, there are a few examples of the reduction of lanthanum (III) to lanthanum metal in 1-octyl-1-methyl-pyrrolidinium bis(trifluoromethylsulfonyl)imide (OMPTf<sub>2</sub>N).<sup>22</sup> The IL utilized is not commercially available and has not been extensively investigated for the deposition of f-elements. In addition, the IL has low conductivity and high viscosity which limits its use in electrochemical experiments.<sup>22</sup>

Finally, the purification of uranium and plutonium metal through electrorefining process with IL has been investigated.<sup>18</sup> The goal of the research was to refine spent nuclear fuels using molten salts which are a form of ionic liquid. The process has been termed pyroelectrochemical processing where the fuel is utilized as the anode and oxidized to dissolve the species in the molten salt. Finally the metals are collected at a Mg cathode of pure metal.<sup>18</sup> The molten salt is not ideal in comparison to room temperature IL system. First, there is a large energy input to maintain the molten salt technology when utilized in the processing of spent nuclear fuel rods. However, the energy cost can be lowered by replacing the molten salt with IL.<sup>18</sup> In addition, the system is highly caustic requiring specialized equipment. Finally, there is often toxic off gas due to side reactions in the molten salt.

The limitations associated with the previous electrochemical studies of f-element dissolution and recovery must be addressed for IL systems to be useful. Care must be taken to assure that the cation/anion pair are stable over the range of electrochemical potentials required to recover the species as metal. Water must be limited in the IL and the metal complexes utilized for dissolution if metals are targeted.

### 1.3 Metal dissolution

The solubility of metal salts in IL has been extensively studied based on the properties of ILs (e.g. low vapor pressure and high chemical stability).<sup>23</sup> Although the physical properties of ILs

are favorable in terms of stability, they hinder the dissolution of metal species. The lack of wettability associated with ILs makes them poor solvents. This extends to the solubility of the inorganic ionic compound such as sodium chloride.<sup>18</sup> In addition, solubility is diminished due to the poor solvating ability of IL with weakly coordinating anions like  $[\text{BF}_4]^-$ ,  $[\text{PF}_6]^-$ , or  $[\text{Tf}_2\text{N}]^-$ .<sup>18</sup> For comparison, metal salts have better solubility in ILs with coordinating anions, such as chloride.<sup>18</sup> Previous studies have demonstrated that lanthanide and actinide salts are more soluble in chloroaluminate in comparison to second generation ILs.<sup>18</sup> Although solubility is higher in  $\text{AlCl}_3$  based ILs, such as 1-ethyl-3-methylimidazolium chloride and aluminum chloride ( $[\text{C}_2\text{mim}]\text{Cl}-\text{AlCl}_3$ ) and 1-butylpyridinium chloride and aluminum chloride ( $\text{BPC}-\text{AlCl}_3$ ), they are water sensitive and can create HCl gas in the presence of water.<sup>23</sup>

An alternative approach for dissolving metal salts in ILs can be utilized with less water sensitive ILs, such as 1-alkyl-3-methylimidazolium hexafluorophosphates ( $[\text{C}_n\text{mim}][\text{PF}_6]$ ), 1-alkyl-3-methylimidazolium tetrafluoroborates ( $[\text{C}_n\text{mim}][\text{BF}_4]$ ), and 1-alkyl-3-methylimidazolium bis(trifluoromethylsulfonyl)-imides ( $[\text{C}_n\text{mim}][\text{Tf}_2\text{N}]$ ).<sup>23</sup> The solubility of metal salts in second generation ILs can be enhanced with the addition of water.<sup>18</sup> In addition, coordination of metal species using ligand similar to those observed in ILs can be used to increase solubility. Finally, the solubility of metal salts can be achieved in polar solvents such as water and ethanol first. In many cases the soluble metal can be directly extracted into the IL by simply mixing the solutions. Alternatively the metal solution can be mixed with the IL and the solvent can be removed using a rotary evaporator.<sup>18</sup> Finally, the solubility of metal salts in ILs contain specific functional groups that assist in the dissolution. For example, a task specific ionic liquid (TSIL) can contain acid functional groups that enhance the metal-salt solubility.<sup>18</sup> However, the functional group must have the ability to coordinate to the metal ion, to facilitate the dissolution of the metal species in



the IL.<sup>23</sup> TSILs are typically mixed with more common ILs because they have a higher melting point, higher viscosity, and are more expensive.<sup>23</sup> The lack of commercially available TSIL remains a drawback to their widespread use and applications.<sup>23</sup>

### 1.3.1 f-element metal dissolution

The solubility of  $\text{LaCl}_3$  in different imidazolium ILs has been previously studied.<sup>24</sup> The data show that  $\text{LaCl}_3$  is slightly soluble in 1-n-butyl-3-methylimidazolium hexafluorophosphate,  $[\text{C}_4\text{mim}][\text{PF}_6]$ .<sup>24</sup> They also found that more  $\text{LaCl}_3$  is dissolved in  $[\text{C}_4\text{mim}][\text{BF}_4]$  in comparison to  $[\text{C}_4\text{mim}][\text{PF}_6]$ .<sup>24</sup> Similarly, studies that have examined dysprosium (III) triflate show that it is slightly soluble in  $[\text{C}_4\text{mim}][\text{PF}_6]$ , and more soluble in  $[\text{C}_4\text{mim}][\text{BF}_4]$ .<sup>18</sup> The data suggests that different anions can be utilized to influence solubility. Similarly, adding ether or hydroxyl functional groups in the alkyl chain of the IL's cation can be utilized to increase solubility.<sup>18</sup> However, regardless of the changes in functional groups in the IL the solubility of f-elements such as  $\text{LaCl}_3$  is low.

The solubility of a wide variety of cerium salts were examined using imidazolium based IL. Among the following cerium salts: ammonium hexanitratocerate (IV), cerium (IV) sulfate dihydrate, cerium (IV) ammonium sulfate, cerium (IV) ammonium sulfate dihydrate, cerium (IV) hydroxide, cerium (IV) triflate, and hydrated cerium (IV) triflate, only ammonium hexanitratocerate (IV) and the cerium (IV) triflate salts demonstrated good solubility in imidazolium based IL.<sup>18</sup> The results suggest that triflate based IL may be used for cerium (IV) dissolution.<sup>18</sup> In addition, rare earth metal oxides were also found to have great solubility in the TSIL protonated betaine bis(trifluoromethylsulfonyl)imide,  $[\text{Hbet}][\text{Tf}_2\text{N}]$ .<sup>18</sup> The increase in solubility in the TSIL is due to the acid-base reaction between the protonated betaine and the rare

earth metal oxide which is facilitated by proton dissociation in residual water in the system. Dissolution results in the formation of the  $[\text{Ln}(\text{bet})_3]\text{-}[\text{Tf}_2\text{N}]$  complex.<sup>18</sup>

A common ion approach has also been utilized to increase the solubility of f-elements in ILs. For example, higher concentrations of f-element dissolved in solution, moisture-sensitive melts, have been achieved based on the formation of bis(trifluoromethylsulfonyl)imide anion ( $\text{Tf}_2\text{N}$ )<sup>-</sup> complexes with actinides and lanthanides.<sup>21</sup> To create  $\text{Tf}_2\text{N}$  complexes, lanthanide oxides are mixed with an aqueous solution of  $\text{HTf}_2\text{N}$  while stirring at  $80^\circ\text{C}$ .<sup>25</sup> This solution is then dried under vacuum at  $200^\circ\text{C}$  for 48 hours.<sup>25</sup> The resulting crystal,  $\text{Ln}(\text{Tf}_2\text{N})_3\cdot 3\text{H}_2\text{O}$  is then dissolved in an IL containing the same anion. The goal is to provide sufficient concentrations of f-element complexes in the IL than can be used for the electrochemical recovery of lanthanide and actinide metals. The ultimate goal is to develop a system for electrochemically refining f-element metals.<sup>21</sup>

#### 1.4 Optical spectroscopy of f-elements in ILs

IL solutions provide a stable environment for monitoring the dissolution and reaction of chemical species including lanthanides and actinides.<sup>26</sup> Very little is known about the solvation of lanthanides and actinides in  $\text{Tf}_2\text{N}$  based ILs, but there is a high interest in using them as substitutes for volatile organic solvents currently used in the reprocessing for spent nuclear fuel.<sup>27</sup> Among the absorption spectra of lanthanide species that have been studied are europium, samarium, and ytterbium, due to the fact that  $\text{Ln}^{3+}$  ions are employed as surrogates for the minor actinides found in spent nuclear fuel (e.g.  $\text{Am}^{3+}, \text{Cm}^{3+}$ ).<sup>27</sup> Specifically, the optical properties of f-elements dissolved in IL can be examined using UV-Vis spectroscopy.  $\text{Ln}^{3+}$  species absorption spectra typically show narrow absorbance bands due to the transitions associated with the 4f valence shell. In addition, broad bands associated with d-group electronic transitions can be observed in the absorbance spectra.<sup>27</sup> The spectra associated with  $\text{Eu}^{2+}$  species are two broad bands at 256 and 313

nm associated with the  $4f^{65d} \leftarrow 4f^7$  transitions.<sup>27</sup> The spectra is similar to those reported for  $\text{Eu}^{2+}$  in acetonitrile and aqueous solutions.<sup>27</sup> Oxidation of  $\text{Eu}^{2+}$  species to  $\text{Eu}^{3+}$  has no observable absorption bands because  $4f \leftarrow 4f$  transitions are too weak to be observed in a smaller molar concentration of  $\text{Eu}^{3+}$  in solution.<sup>27</sup>

Alternatively, there is very little UV-Vis data associated with actinides species in IL, with the exception of  $\text{UO}_2^{2+}$ . The recovery of plutonium and uranium through the PUREX process produces the soluble oxidized actinide species in aqueous solution. ILs have been suggested as a solvent for the extraction of actinide species over lanthanide species.<sup>28</sup> Therefore, dioxouranium (VI) ion (uranyl ion,  $\text{UO}_2^{2+}$ ) is the most common species encountered for both experimental and theoretical studies involving uranium. Likewise, the study of  $\text{UO}_2(\text{Tf}_2\text{N})_2 \cdot x\text{H}_2\text{O}$  in  $[\text{C}_6\text{mim}][\text{Tf}_2\text{N}]$  and  $\text{UO}_2(\text{ClO}_4)_2 \cdot x\text{H}_2\text{O}$  in  $[\text{C}_4\text{mim}][\text{Tf}_2\text{N}]$  or  $[\text{C}_4\text{mpyr}][\text{Tf}_2\text{N}]$  has been conducted. The  $[\text{Tf}_2\text{N}]^-$  and  $\text{ClO}_4^-$  anions are weakly coordinating anions and do not extensively coordinate with the uranyl ion in the presence of other stronger ligating species.<sup>28</sup> Therefore, UV-Vis absorption spectra show the same features regardless of the uranyl salt that is dissolved, or the different ILs that were used.<sup>28</sup> The residual water in the IL results in the conversion of the salts to the fully hydrated form.<sup>28</sup> In each case, water molecules coordinated with the uranyl ion,  $[\text{UO}_2(\text{H}_2\text{O})_5^{2+}]$ , even for ILs with water content below 100ppm. The data shows that water is a better ligand even at low concentration when compared to the weakly binding  $[\text{Tf}_2\text{N}]^-$  anion which does not coordinate with the uranyl ion.<sup>28</sup>

## 1.5 Motivation

Green chemistry is referred to as the prevention of waste, as opposed to having to clean it up. If products must be synthesized, it should possess little to no toxicity to the human health and environment. The rare-earth elements (REEs) are becoming more important in the attempts to have

a greener economy. For example, REEs play a significant role due to their applications and compositions in permanent magnets, lamp phosphors, catalysts, and rechargeable batteries.<sup>29</sup> Wind turbines, hybrid and electric cars, and compact fluorescent lamps have increased the demand and the price of REEs.<sup>29</sup> China currently dominates the market and manufactures more than 90% of the global REE that is on the market.<sup>29</sup> There is currently a push in the US and other countries to develop mining and refining capabilities. Mining companies all over the world are in search of exploitable REE deposits and old mines are reopening for business to minimize the Chinese dominance of the market.<sup>29</sup> However, the lack of economical and operational mineral mining areas has shifted the focus from mining to the recycling of REEs from industrial residues, pre-consumer scrap, and End-of-Life products.<sup>29</sup> Recycling already mined metals is preferred in order to prevent the excess of more abundant elements.<sup>29</sup> For example, ores for neodymium also contains lanthanum and cerium, both of which are already in excess.<sup>29</sup> According to the U.S. Department of Energy (DOE), the five most critical REEs are: neodymium, europium, terbium, dysprosium, and yttrium.<sup>29</sup> Recycling decreases the amount of REE ores that have to be extracted and refined.<sup>29</sup> However, in 2011, only less than 1% of REEs were recycled due to lack of incentive to recycle, inefficient collection, and technological problems.<sup>29</sup> Efficiency in recycling is necessary in order to capitalize on the REE that is stockpiled in recycling centers and landfills, especially now that China has decided to tighten their export quota from 50,145 tons in 2009 to 31,130 tons in 2012.<sup>29</sup> More importantly, the demand in the next 25 years is estimated to rise up to 700% for neodymium and 2600% for dysprosium.<sup>29</sup> The market limitations imposed by Chinese control of the REE market suggests that recycling will become increasingly important. Therefore, methods for the recovery and refining of lanthanide metals are of strategic and scientific importance.

## 1.6 Present studies (hypothesis)

The hypothesis of the current thesis is that the direct dissolution of Sm and Eu carbonates can be achieved in IL solutions producing soluble metal species at sufficient concentrations to facilitate the electrochemical recovery of metal. The direct dissolution and electrochemical recovery of lanthanide metal species Sm and Eu is examined. Specifically, the method of dissolution employed in the present studies will allow the electrochemical deposition of samarium and europium metal species from IL solutions. The direct dissolution of both Sm and Eu into IL is utilized rather than the formation of aqueous complexes to minimize the impact of water on the electrochemical deposition processes.

## Chapter 2. Experimental Methods

This chapter will serve as background information about the methods and instruments that were used to perform the research. The dissolution data for samarium carbonate and europium carbonate are provided. Each subsequent chapter will go into further detail as well as the parameters relevant to the research.

### 2.1 Dissolution methods: Comparison of previous methods with direct dissolution

Other works pertaining to lanthanide depositions have been abundant in literature. Studies on lanthanum deposition has been researched, but the resulting deposition is an aluminum-lanthanum alloy, based on the IL solvent used.<sup>30,31</sup> The work focuses on first generation aluminum chloride ionic liquids that have high water sensitivity. Thus, the acidity and basicity of the chloroaluminate IL used influence the dominating species formed with anionic (in a basic environment) or cationic (in an acidic environment) dominating. Deposition of neutral metal is difficult and rarely achieved due to the speciation observed in chloroaluminate IL.<sup>18</sup> Previously, dysprosium deposition studies also resulted in a  $\text{DyCl}_3$  alloy with  $\text{CoCl}_2$ .<sup>18</sup> A study of  $\text{NdCl}_3$  showed low solubility in  $[\text{C}_2\text{mim}][\text{Cl}]$  based IL and a comprehensive study proved to be challenging.<sup>32</sup> Finally, the study of europium in  $[\text{C}_4\text{mim}][\text{Tf}_2\text{N}]$  IL showed water molecules coordinate to the  $\text{Eu}^{3+}$  preferentially in comparison to the  $[\text{Tf}_2\text{N}]^-$  anion.<sup>33</sup> Other studies using different ILs such as fluorinated anions and hexafluorophosphate anion are likely to undergo hydrolysis, which can cause the formation of toxic byproducts such as hydrogen fluoride.<sup>34</sup>

Indirect dissolution of lanthanide metals utilized aqueous systems and hydrated crystals which can be incorporated into the IL. The method overcomes the solubility barrier of the IL. Hydrated crystals such as  $\text{Th}(\text{Tf}_2\text{N})_4(\text{HTf}_2\text{N})\cdot 2\text{H}_2\text{O}$ ,  $\text{Ln}(\text{Tf}_2\text{N})_3(\text{HTf}_2\text{N})\cdot 3\text{H}_2\text{O}$ ,  $\text{Eu}(\text{Tf}_2\text{N})_3(\text{HTf}_2\text{N})\cdot 3\text{H}_2\text{O}$ , and  $\text{Sm}(\text{Tf}_2\text{N})_3(\text{HTf}_2\text{N})\cdot 3\text{H}_2\text{O}$  have all been previously reported in literature.<sup>20, 21</sup> However, all

deposits recovered from this dissolution method have been attributed to lanthanide oxides, due to reaction with water. No elemental metal lanthanide deposits were obtained from the dissolution of hydrated complexes. Direct dissolution of IL eliminates the use of hydrated species and utilizes the weakly coordinated  $\text{Tf}_2\text{N}$  to complex with minimal interaction with water. The method utilizes the direct dissolution of lanthanide carbonate species which produce carbonic acid which can be removed through degassing or rotary evaporation under vacuum. The concentration of the anion in the IL provides a favorable environment for complexation with  $\text{TF}_2\text{N}$  rather than any residual water produced in the dissolution and decomposition of carbonic acid.

## 2.2 Materials

The N-trimethyl-N-butylammonium bis(trifluoromethylsulfonyl)imide  $[\text{Me}_3\text{N}^n\text{Bu}][\text{Tf}_2\text{N}]$  IL was obtained from Solvionic (99.5%). The  $\text{HTf}_2\text{N}$ , N,N-bis(trifluoromethylsulfonyl)imide, is an acid with the same anion ( $\text{Tf}_2\text{N}^-$ ) contained in the IL. It was obtained from SynQuest Labs (99%). Ultrapure water from a Barnstead E-pure system ( $\sim 18\Omega$ ) was utilized for the aqueous synthesis of the lanthanide complexes. samarium (III) carbonate hydrate,  $\text{Sm}_2(\text{CO}_3)_3 \cdot x\text{H}_2\text{O}$ , was obtained from Alfa Aesar (99.99%) and the europium (III) carbonate hydrate,  $\text{Eu}_2(\text{CO}_3)_3 \cdot x\text{H}_2\text{O}$  was obtained from Strem Chemicals (99.9%).

### 2.2.1 Samarium Dissolution

The dissolution of samarium carbonate was initiated by mixing 10mL of IL  $[\text{Me}_3\text{N}^n\text{Bu}][\text{Tf}_2\text{N}]$  and 1.5mL of ultrapure water to form a “wet” IL solution. The solution was then sonicated to fully incorporate the water throughout the IL, and then 0.3606g of samarium carbonate ( $\text{Sm}_2(\text{CO}_3)_3 \cdot x\text{H}_2\text{O}$ ) (0.150M  $\text{Sm}^{3+}$ ) was added. The solution was then sonicated again to disperse the samarium carbonate uniformly into the “wet” IL. An additional 5mL of ultrapure water was added to form a phase separation and fully saturate the samarium carbonate “wet” IL solution. The

solution was then left untouched for 24 hours and the water layer was manually removed by pipette. The dissolution of the samarium carbonate suspended in the IL was achieved by adding 1.5350g of HTf<sub>2</sub>N (0.545M) and placing in the sonicator. The samarium carbonate dissolved within a 24-hour window producing a clear solution. The acidic solution is then mixed with water and shaken. Once the solution has settled, the water is pipetted out and the pH is measured with pH strips. The addition of water is to remove as much of the HTf<sub>2</sub>N as possible. This procedure is repeated until the pH strip results in a more neutral pH and no more pH change is occurring. The resulting solution is purged with dry nitrogen for at least six hours to remove the water from the IL solution containing dissolved Sm.

### 2.2.2 Europium Dissolution

The dissolution of europium carbonate was initiated by mixing 10mL of IL [Me<sub>3</sub>N<sup>m</sup>Bu][Tf<sub>2</sub>N] and 1.5mL of ultrapure water to form a “wet” IL solution. The solution was then sonicated to fully incorporate the water throughout the IL, and then 0.3620g of europium carbonate (Eu<sub>2</sub>(CO<sub>3</sub>)<sub>3</sub>·xH<sub>2</sub>O) (0.150M Eu<sup>3+</sup>) was added. The solution was then sonicated again to disperse the europium carbonate uniformly into the “wet” IL. An additional 5mL of ultrapure water was added to form a phase separation and fully saturate the europium carbonate “wet” IL solution. The solution was then left untouched for 24 hours and the water layer was manually removed by pipetting. The dissolution of the europium carbonate suspended in the IL was achieved by adding 1.9794g of HTf<sub>2</sub>N (0.704M) and placing in the sonicator. The europium carbonate dissolved within a 24-hour window producing a clear solution. The acidic solution is then mixed with water and shaken. Once the solution has settled, the water is pipetted out and the pH is measured with pH strips. The addition of water is to remove as much of the HTf<sub>2</sub>N as possible. This procedure is repeated until the pH strip results in a more neutral pH and no more pH change is occurring. The



resulting solution is purged with dry nitrogen for at least six hours to remove the water from the IL solution containing dissolved Eu.



**Figure 3.** Lanthanide dissolution: Lanthanide carbonate→IL addition→H<sub>2</sub>O addition→shaken mixture→after the addition of HTf<sub>2</sub>N

### 2.3 Acid neutralization and water removal

Acid neutralization and water removal is crucial in electrochemistry as both acid and water will hinder deposition. To remove as much acid as possible, a liquid-liquid extraction was performed on the solution with soluble lanthanide metal. Ultra-pure water was added into the solution, and then thoroughly mixed. The solution was allowed to settle until a phase separation occurred. Once the two phases have separated, the aqueous layer was manually taken out with a pipette. The aqueous layer was then poured into a beaker and a pH paper was utilized to measure the pH of the aqueous layer. These procedures were repeated until the pH paper no longer showed drastic changes in pH (**Figure 4**). Once excess acid was removed from the IL solution, the residual water was removed via the use of a rotary evaporator at 25 mbar and 50 °C to bring the solution back to its pristine form.

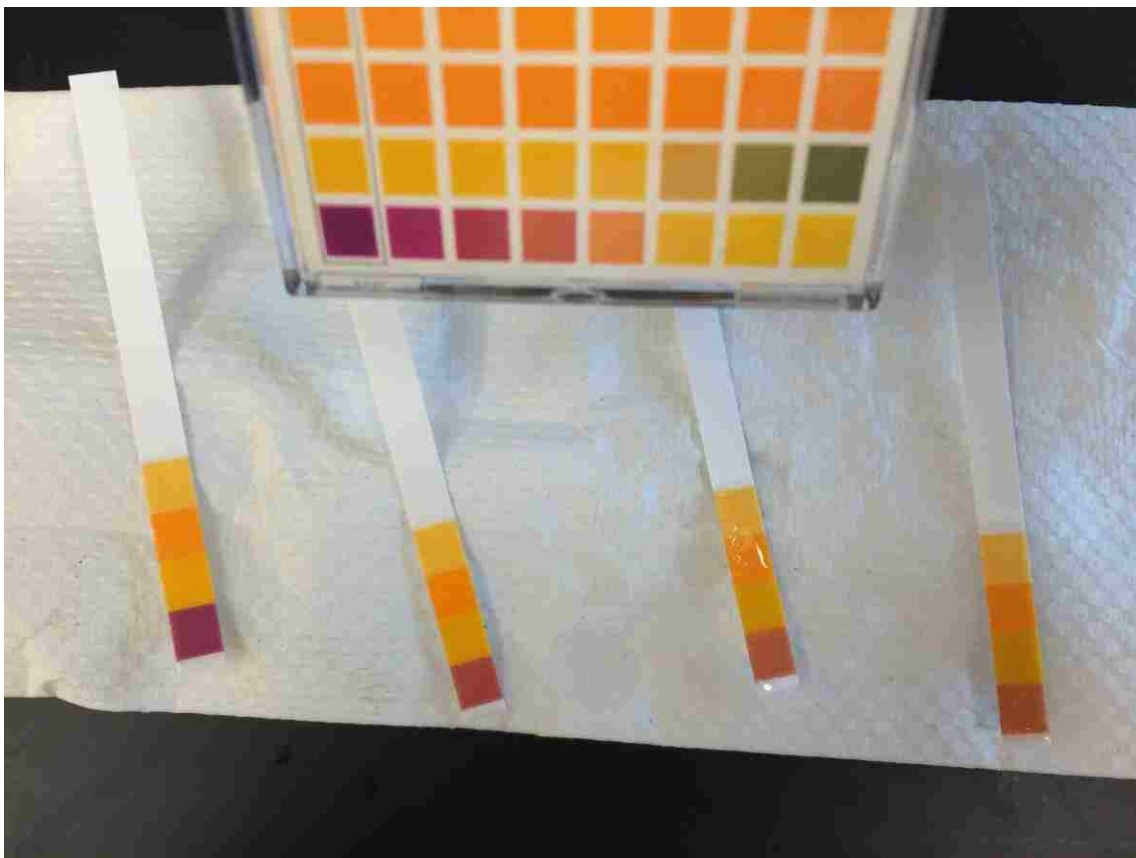


**Figure 4.** pH of aqueous layer started at 1, but became less acidic as the process was repeated.

## 2.4 Spectroscopy

UV-Vis spectroscopy was utilized to evaluate the dissolved Sm and Eu in the IL solutions. The lanthanide species have d-f transitions in the visible range that can be measured. Ultraviolet-visible (UV-Vis) spectroscopy is a type of electronic spectroscopy that measures absorption of electromagnetic radiation by molecules and atoms as a function of the wavelength. As the light passes through a solution containing a target species, light is absorbed by molecules which excites electrons from an occupied orbital to an unoccupied orbital. The electronic transition depends on the atom or molecule that is being examined. The absorption of electromagnetic radiation can be monitored as a function of the intensity of light transmitted through the sample. The relationship between transmittance and absorbance is based on a simple relationship provided below.

Typically, absorbance spectra provide valuable information about the molecule or atoms' electronic energy levels and oxidation states.

The UV-Vis spectrophotometer measures the intensity of light transmitted through a sample,  $I$ , and compares it to the incident intensity from a reference material,  $I_0$ . The ratio  $I/I_0$  is the transmittance,  $T$ . The instrument provides the absorbance,  $A$ , based on the negative log of the transmittance.<sup>35</sup>

$$A = -\log I/I_0 = -\log T \quad \text{Equation 5.}$$

The Beer-Lambert Law gives the linear relation between the concentration of the species and the absorbance.<sup>35</sup>

$$A = -\log T = \epsilon bc \quad \text{Equation 6.}$$

The molar absorptivity ( $\epsilon$ ,  $L \text{ mol}^{-1} \text{ cm}^{-1}$ ) is both species and matrix dependent. The path length ( $b$ ,  $\text{cm}$ ) is a known constant based on the cuvette that is being used and is typically 1  $\text{cm}$ . Finally, the molar concentration ( $c$ ,  $\text{mol L}^{-1}$ ) is used in the equation. The UV-Vis spectra were collected through Cary 100 UV-Vis Spectrometer using quartz cuvettes under normal conditions. Absorbance spectra were collected using IL with no analyte for use as a reference background for subtraction.

## 2.5 Electrochemistry

### 2.5.1 Cyclic Voltammetry

The standard reduction potentials for electrochemical reactions in aqueous solutions are typically reported versus a normal hydrogen electrode (NHE, also known as the “Standard Hydrogen Electrode” or SHE) or versus a saturated Ag/AgCl reference electrode. SHE has a standard electrode potential  $E^0$  of 0 V.<sup>36</sup> Therefore, all cathodic reduction reactions are listed

versus the NHE or SHE anode where  $E_{\text{cell}} = E_{\text{cathode}} - E_{\text{anode}}$ . The value of  $E_{\text{cell}}$  is equal to  $E_{\text{cathode}}$  for NHE and SHE.

The primary electrochemical method utilized in this thesis is cyclic voltammetry. The cell set up for the electrochemistry is important because it requires the working electrode to function as both cathode or anode depending on the applied potential. A three-electrode cell is utilized to ensure that the reference electrode does not react and change potential during potential cycling. The system includes a working electrode (e.g. Au, Pt, Ag, GC, grafoil), a counter electrode (Pt), and a reference electrode which is described in more detail below. The working electrodes used in this experiment are glassy carbon (GC) and grafoil. The GC electrode must be cleaned with alumina powder on a microcloth pad and rinsed with ultra-pure water prior to running electrochemistry. The grafoil comes from a sheet of grafoil paper and is cut into a smaller piece in order to fit into the electrochemical cell. No prior steps need to be done on the grafoil sheet. The reference electrode is used to control the applied potential to the working electrode. However, the counter is used to pass current based on oxidation/reduction processes at the working electrode. The current is passed between the working and counter electrode to ensure the composition and potential of the reference electrode remains unchanged during electrochemical reactions.

In the current studies, the solvent system is non-aqueous IL. Therefore, the reference electrode is constructed with IL solvent, a silver wire, and  $\text{Ag}^+$  to produce a non-aqueous  $\text{Ag}/\text{Ag}^+$  reference electrode. An  $\text{Ag}/\text{Ag}^+$  (0.1 M  $\text{AgNO}_3$  in IL) non-aqueous reference electrode was created for this purpose based on the literature by Saheb, et al.<sup>37</sup> First,  $\text{AgNO}_3$  must be dissolved in acetonitrile. Once all of the  $\text{AgNO}_3$  were fully dissolved, 0.1 M of  $\text{Ag}^+$  is measured and mixed into the IL solution. This  $\text{Ag}^+$  solution is transferred into a glass electrode and is put in contact with an Ag wire.

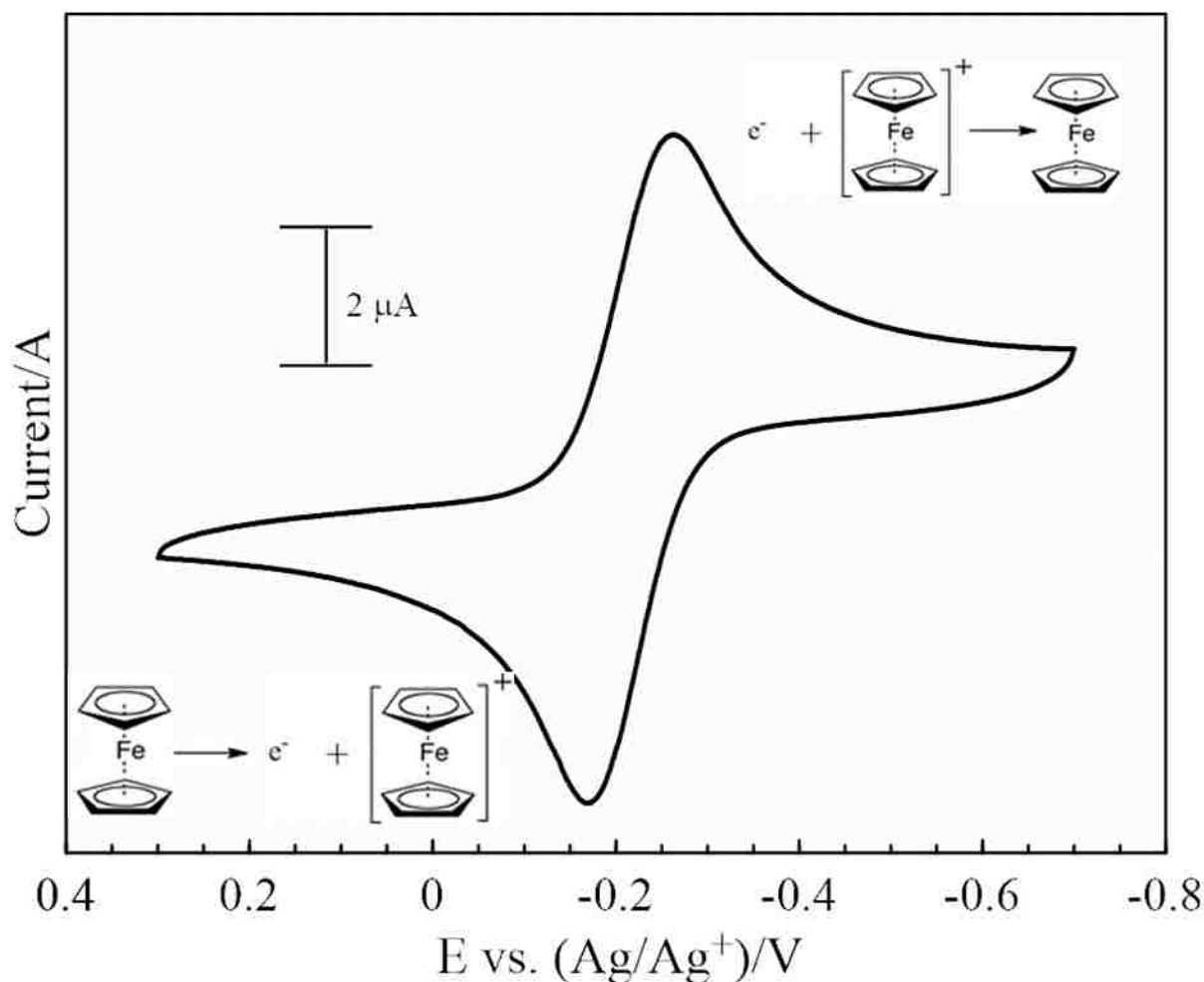


**Figure 5.** Cyclic voltammetry of 5 mM ferrocene in [Me<sub>3</sub>N<sup>n</sup>Bu][Tf<sub>2</sub>N].

The reference electrode required calibration using a standard oxidation/reduction process to determine the potential offset versus the NHE electrode or Ag/AgCl electrode discussed previously. The redox potentials of the ferrocene/ferrocenium (Fc/Fc<sup>+</sup>) in IL can be compared directly with species in aqueous system to determine the offset. For example, the literature<sup>13, 36</sup> states that redox potential for Fc/Fc<sup>+</sup> couple is +0.400 V versus SHE or +0.201 V versus saturated Ag/AgCl.<sup>13</sup> The Ag/Ag<sup>+</sup> in IL reference electrode was occasionally standardized in a solution containing about 5 mM ferrocene dissolved directly in IL with no water or acid added. The typical reduction for the ferrocene occurs at -0.263 V, giving an offset value of +0.464 V versus Ag/AgCl. Therefore, this value must be added to any potential obtained using the Ag/Ag<sup>+</sup> electrode to

represent the reaction versus the Ag/AgCl reference. This becomes increasingly important if we want to compare the oxidation/reduction of lanthanides to the known values for Hg amalgamation in aqueous solutions. All electrochemistry data were collected using CH Instruments potentiostat 760C. The working electrodes used were gold disc, glassy carbon disc, and grafoil. Platinum is the choice for counter electrode as it is a great electron source. A non-aqueous Ag/Ag<sup>+</sup> (0.1M Ag<sup>+</sup> in IL) reference electrode was used. Two reference electrodes were utilized in the study: one for background and one for the metal to avoid contaminating the background solutions.

Controlled potential processes such as cyclic voltammetry (CV) are techniques that can be used to probe the oxidation/reduction of molecules at a working electrode. In addition, the methods can be used for the controlled electrochemical plating of metal species. Deposition of chemical species including metal cations occurs as the cathodic scan reaches sufficient negative potential to result in the reduction of the cation to metal at the electrode surface. If the potential is cycled to more positive potentials, it is possible to re-oxidize the metal deposits to remove them from the cathode. However, in the case of most f-elements the oxidation potential required to fully remove metal deposits is not typically achieved. In most cases the potential is simply poised at a negative potential to achieve metal deposition and the potential is never cycled back to more positive values.

### 2.5.2 Amperometric Deposition

Amperometric i-t Curve is another electrochemistry technique that was utilized in order to electrodeposit more efficiently onto the working electrode. Amperometry deposition is the application of a constant potential over a certain period of time (also known as chronoamperometry). After the cyclic voltammetry is scanned, the given potential window's scan reveals where the metal is essentially reduced down into its metal form. This working electrode is held at that potential for a period of 24 hours in order to ensure that electrodeposition has occurred.

The same three electrode system is utilized in the amperometric i-t curve as in the cyclic voltammetry method. Both gold foil and grafoil have flat surfaces that allow the metal to be plated on a flat surface for analysis using SEM/EDX.

## 2.6 SEM/EDX

Scanning Electron Microscopy (SEM) and Energy Dispersive X-ray Spectroscopy (EDX) are analytical methods used to study the surface of the electrodeposited materials. The SEM rasters the electrons using tungsten as an electron source and focuses the electrons into a beam using electromagnetic lenses as it scans through the surface of the sample. The electrons interact with the sample and ejects secondary electrons, backscattered electrons, as well as characteristic x-rays which are detected by the detector and reveals an image of the surface. These electrons are also used by the EDX in order to reveal the chemical composition of the sample. The SEM is used to look at the surface of the of the gold foil and grafoil. Since the samples are metals and, therefore, electrically conductive, the samples did not need to be covered with neither carbon nor gold in the sputter coater. If the samples do not provide their own pathway to ground, the samples would accumulate electrostatic charge which will cause scanning faults and various image artifacts. Each element emits characteristic x-rays which the EDX is able to distinguish. These x-ray signals can be used to map the abundance of the elements as well. SEM data were collected using JEOL-5610 scanning electron microscope equipped with a secondary electron and backscatter electron detectors. EDX data were collected using INCA mapping software.

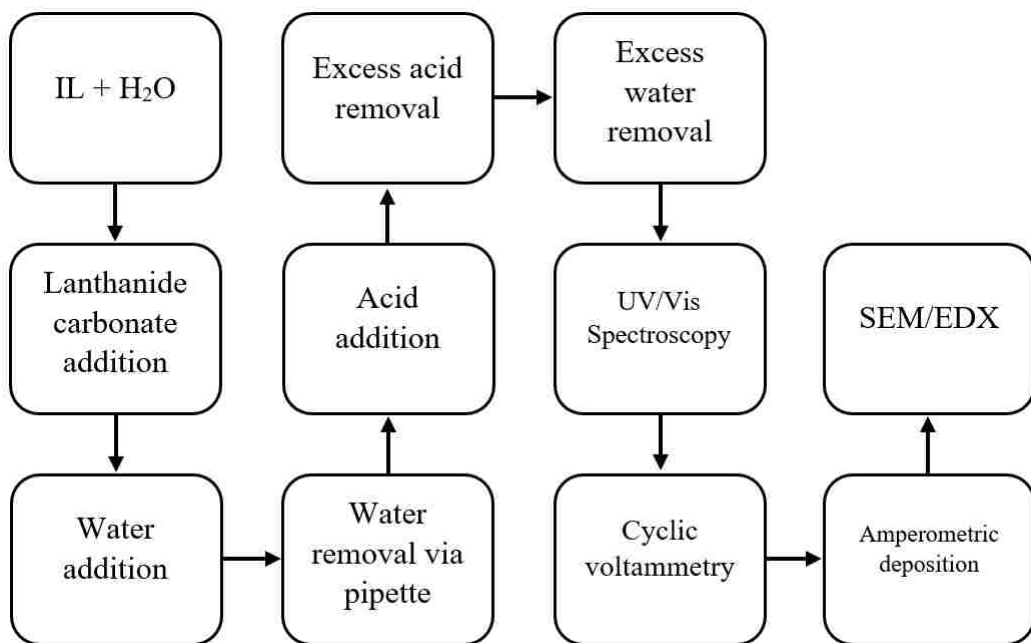


**Figure 6.** Flow diagram for the dissolution and recovery of lanthanide metals.

### Chapter 3. Samarium and Europium Dissolution and Electrochemistry

#### 3.1 Introduction

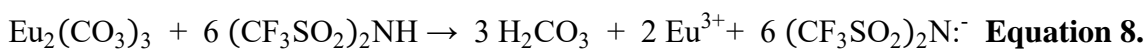
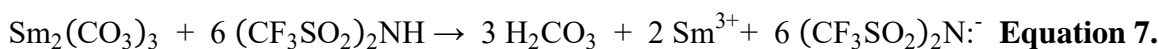
This chapter examines the dissolution of the lanthanide carbonates directly into the IL solution with the addition of acid,  $\text{HTf}_2\text{N}$ . The soluble lanthanide species were analyzed using UV-Vis spectroscopy and using electrochemical methods. The reduction and oxidation of the dissolved



lanthanide metals were evaluated, and the electrochemical deposition of the lanthanides were explored using cyclic voltammetry and amperometry methods. SEM and EDX analysis were used to confirm the recovery of the samarium and europium metals.

### 3.2 Samarium and Europium Dissolution

The dissolution of lanthanide carbonates were achieved using wet IL in the presence of acid, HTf<sub>2</sub>N. The solution concentration that was achieved was 150 mM. The water and acid were added to enhance deprotonation and increase solubility through wetting of the carbonate species by water.<sup>23</sup> The acid facilitated the formation of the carbonic acid intermediate which decomposed to form water and CO<sub>2</sub> which can be easily removed from the IL while achieving the dissolution of samarium and europium into the IL, **Equations 7 and 8**.



The visible dissolution of lanthanide carbonate was apparent when the IL solution turned from cloudy to clear. The clear solution can have two distinct layers: aqueous and organic. The excess water was removed with the use of a rotary evaporator at 50 °C and 25 mbar in order to have a pristine solution of soluble samarium in IL and soluble europium in IL. Once the water was removed, UV-Vis spectroscopy and electrochemistry can be utilized to evaluate the soluble samarium and europium.

#### 3.2.1 UV-Vis Spectroscopy Results

The UV-Vis response of the IL solution containing 150 mM samarium from Sm<sub>2</sub>(CO<sub>3</sub>)<sub>3</sub>·xH<sub>2</sub>O with HTf<sub>2</sub>N and 150 mM europium from Eu<sub>2</sub>(CO<sub>3</sub>)<sub>3</sub>·xH<sub>2</sub>O with HTf<sub>2</sub>N were under ambient conditions. The IL was washed with water to remove any excess acid and dried using a rotary

evaporator to remove the water. The soluble lanthanide species were compared with a plain IL solution as background, **Figure 7 and 8**.

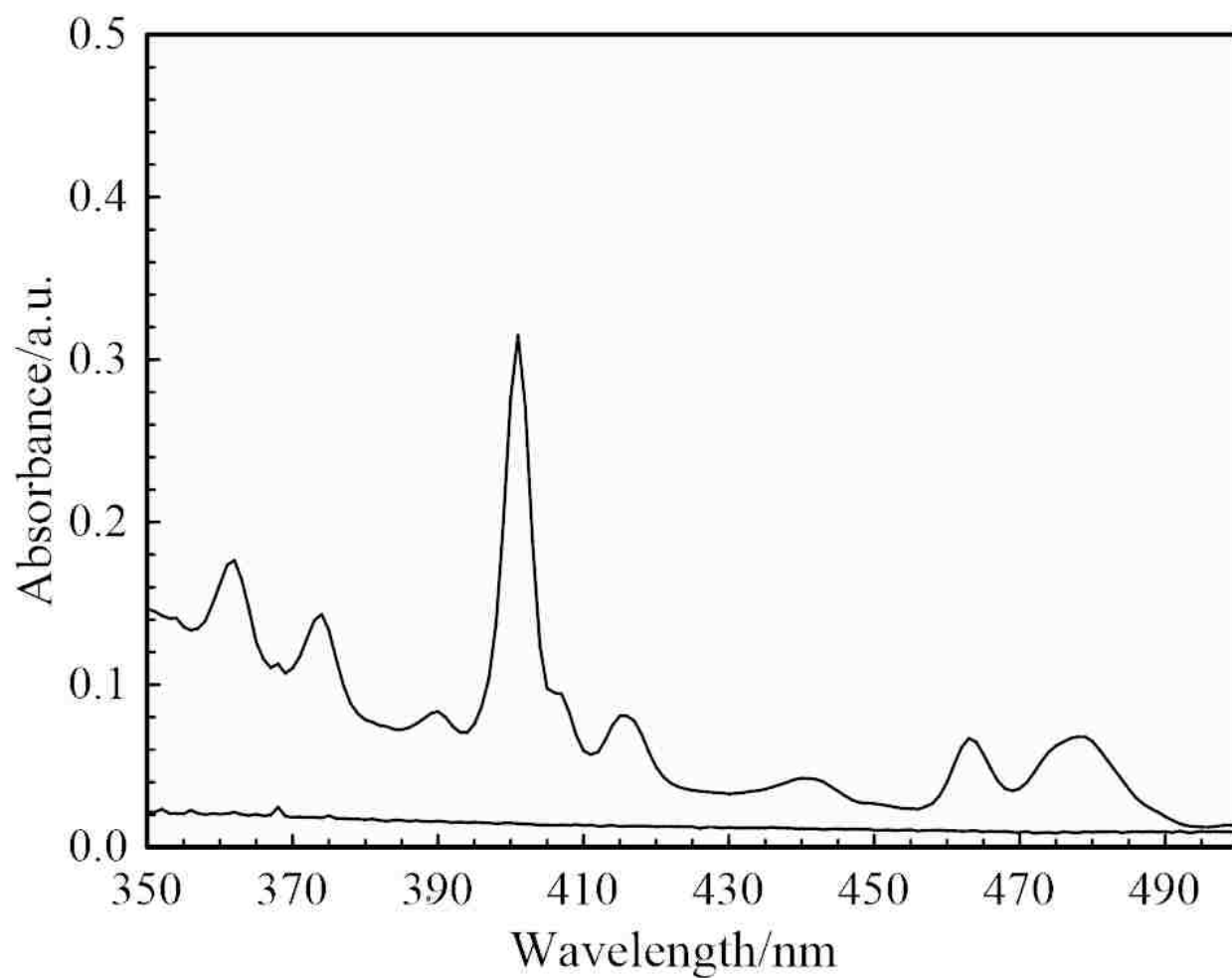


**Figure 7.** UV-Vis absorbance spectra IL,  $[\text{Me}_3\text{N}^{\text{n}}\text{Bu}][\text{Tf}_2\text{N}]$ , and IL containing 150 mM Sm.

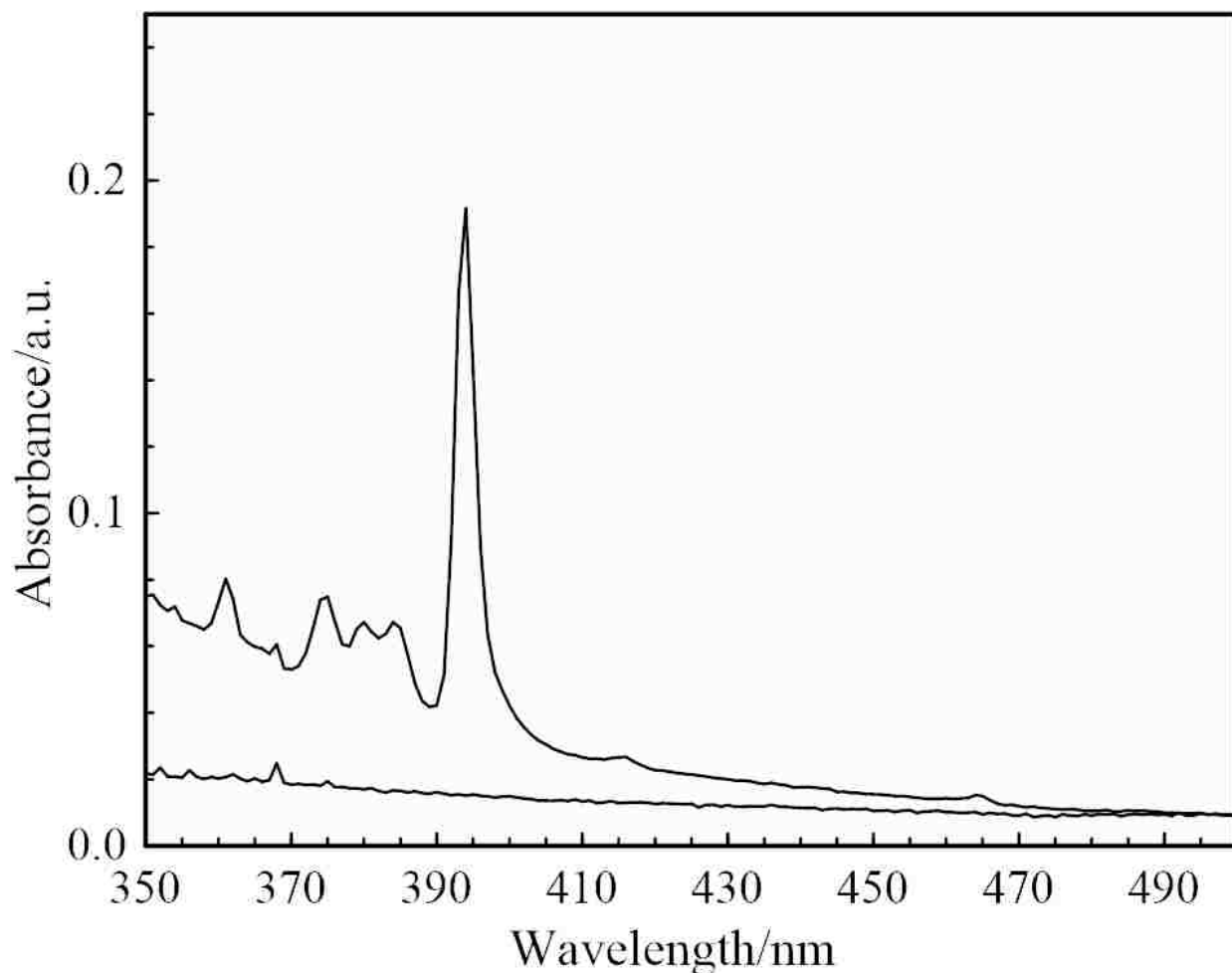


**Figure 8.** UV-Vis absorbance spectra IL,  $[\text{Me}_3\text{N}^n\text{Bu}][\text{Tf}_2\text{N}]$ , and IL containing 150 mM Eu.

The UV-Vis absorbance band associated with the IL shows up between 200 nm to 250 nm. The spectral region between 200 nm to 350 nm is not shown because it shows absorption bands associated with the IL. The absorbance bands associated with the soluble samarium and europium are found between 350 nm and 500 nm which are readily visible against the background IL.

These bands located between 350 nm and 500 nm are associated with the  $4f \rightarrow 4f$  transitions of samarium, since trivalent samarium has five electrons occupying the 4f orbital, while samarium's ground state is  $^6\text{H}_{5/2}$ .<sup>27</sup> The absorbance bands found for samarium is consistent with f-element transitions associated with samarium complexes.<sup>27</sup> These absorbance bands are consistent with those reported in literature. The absorbance fine structure is indicative of multiple electronic

transitions associated with soluble samarium that suggests that  $\text{Sm}(\text{TFSI})_3$  forms during dissolution of samarium in IL with  $\text{HTf}_2\text{N}$ . Absorbance at lower wavelength for lanthanide species can be attributed to ligand to metal charge transfer complexes which have been observed for weakly coordinating ligands.<sup>38</sup> The  $\text{Tf}_2\text{N}$  acts as sensitizing agents, which strongly absorb light and transfer the energy to the metal center, for high energy electronic transitions.<sup>38</sup> The transition states for samarium have been reported and the peaks for this spectrum are assigned as:  ${}^6\text{H}_{5/2} \rightarrow {}^4\text{D}_{3/2}$  at 362 nm,  ${}^6\text{H}_{5/2} \rightarrow {}^4\text{L}_{17/2} + {}^4\text{K}_{17/2}$  at 376 nm,  ${}^6\text{H}_{5/2} \rightarrow {}^4\text{L}_{15/2} + {}^4\text{K}_{15/2}$  at 390 nm,  ${}^6\text{H}_{5/2} \rightarrow {}^4\text{P}_{3/2}$  at 404 nm,  ${}^6\text{H}_{5/2} \rightarrow {}^4\text{M}_{19/2}$  at 417 nm,  ${}^6\text{H}_{5/2} \rightarrow {}^4\text{I}_{15/2} + {}^4\text{M}_{15/2}$  at 442 nm,  ${}^6\text{H}_{5/2} \rightarrow {}^4\text{I}_{13/2} + {}^4\text{K}_{13/2}$  at 466 nm, and  ${}^6\text{H}_{5/2} \rightarrow {}^4\text{I}_{11/2} + {}^4\text{M}_{15/2}$  at 478 nm.<sup>27, 39-41</sup> A  ${}^6\text{H}_{5/2} \rightarrow {}^4\text{F}_{3/2}$  transition has also been assigned at 1563nm<sup>40</sup> for samarium, but the range for our UV-Vis spectrometer does not go beyond 800nm. The spectra for samarium are similar to the known spectra reported to be dissolved in perchloric acid and acetonitrile.<sup>42, 43</sup>

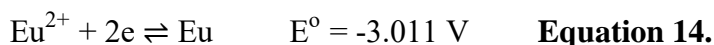
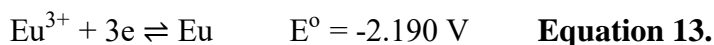
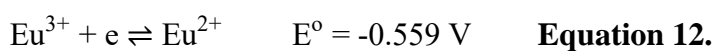
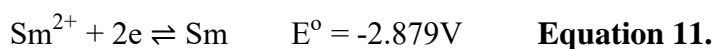
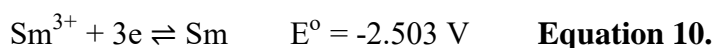
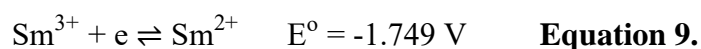
Six electrons occupy trivalent europium's 4f orbital, while its ground state is  ${}^7\text{F}_0$ .<sup>27</sup> The absorbance bands found for europium is consistent with f-element transitions associated with europium complexes.<sup>27</sup> These absorbance bands are consistent with those reported in literature. The absorbance fine structure is indicative of multiple electronic transitions associated with soluble europium that suggests that  $\text{Eu}(\text{TFSI})_3$  forms during the dissolution of europium in IL with  $\text{HTf}_2\text{N}$ . The transition states for samarium have been reported and the peaks for this spectrum are assigned as:  ${}^7\text{F}_0 \rightarrow {}^5\text{D}_4$  at 361 nm,  ${}^7\text{F}_0 \rightarrow {}^5\text{D}_4$  at 375 nm,  ${}^7\text{F}_0 \rightarrow {}^5\text{G}_4$  at 380 nm,  ${}^7\text{F}_0 \rightarrow {}^5\text{G}_2$  at 388 nm,  ${}^7\text{F}_0 \rightarrow {}^5\text{L}_6$  at 395 nm,  ${}^7\text{F}_0 \rightarrow {}^5\text{L}_7$  at 416 nm, and  ${}^7\text{F}_0 \rightarrow {}^5\text{D}_3$  at 464 nm.<sup>27, 39, 40</sup> The spectrum of europium is similar to other reported values for solvated europium species in acetonitrile and aqueous solvents.<sup>43, 44</sup> Other reported europium dissolution in methanol and water also showed similar spectra.<sup>45-47</sup> A slight shift in spectrum can be observed in different ILs, however. Europium bands

have been observed between 290 nm and 355 nm in BuMeIMPF<sub>6</sub> IL, due to a different solvation environment given by the PF<sub>6</sub><sup>-</sup> ion versus the Tf<sub>2</sub>N<sup>-</sup>.<sup>48</sup>

### 3.3 Electrochemistry

#### 3.3.1 Cyclic Voltammetry

The reduction and oxidation of soluble samarium in IL was examined using cyclic voltammetry. As stated previously, the potential window in aqueous solutions are typically hindered by water oxidation or metal oxide formation at the positive potential limiting the ability to study lanthanide species. In addition, residual water in IL can also result in appreciable hydrogen evolution at the negative potentials which limits the reduction of lanthanide metals. Therefore, water acid neutralization and water removal were required to evaluate the reduction of soluble samarium at negative potentials, **Equations 9 through 14**. The potentials<sup>13</sup> required for the reduction of samarium in an aqueous solution versus Ag/AgCl are typically:



In order to evaluate the water in IL, a nondestructive method using a gold disc electrode<sup>49</sup> was utilized. 10 mL of IL was mixed with 10 mL of ultra-pure water. The solutions were mixed in a sonicator and allowed to settle for 24 hours. Using a gold disc electrode, cyclic voltammetry was run on the wet IL solution. The solution was then purged with dry N<sub>2</sub> gas for 4, 6, and 12 hours

and evaluated using cyclic voltammetry. The cyclic voltammetry scans show that purging with N<sub>2</sub> gas brings the IL back to its pristine form.

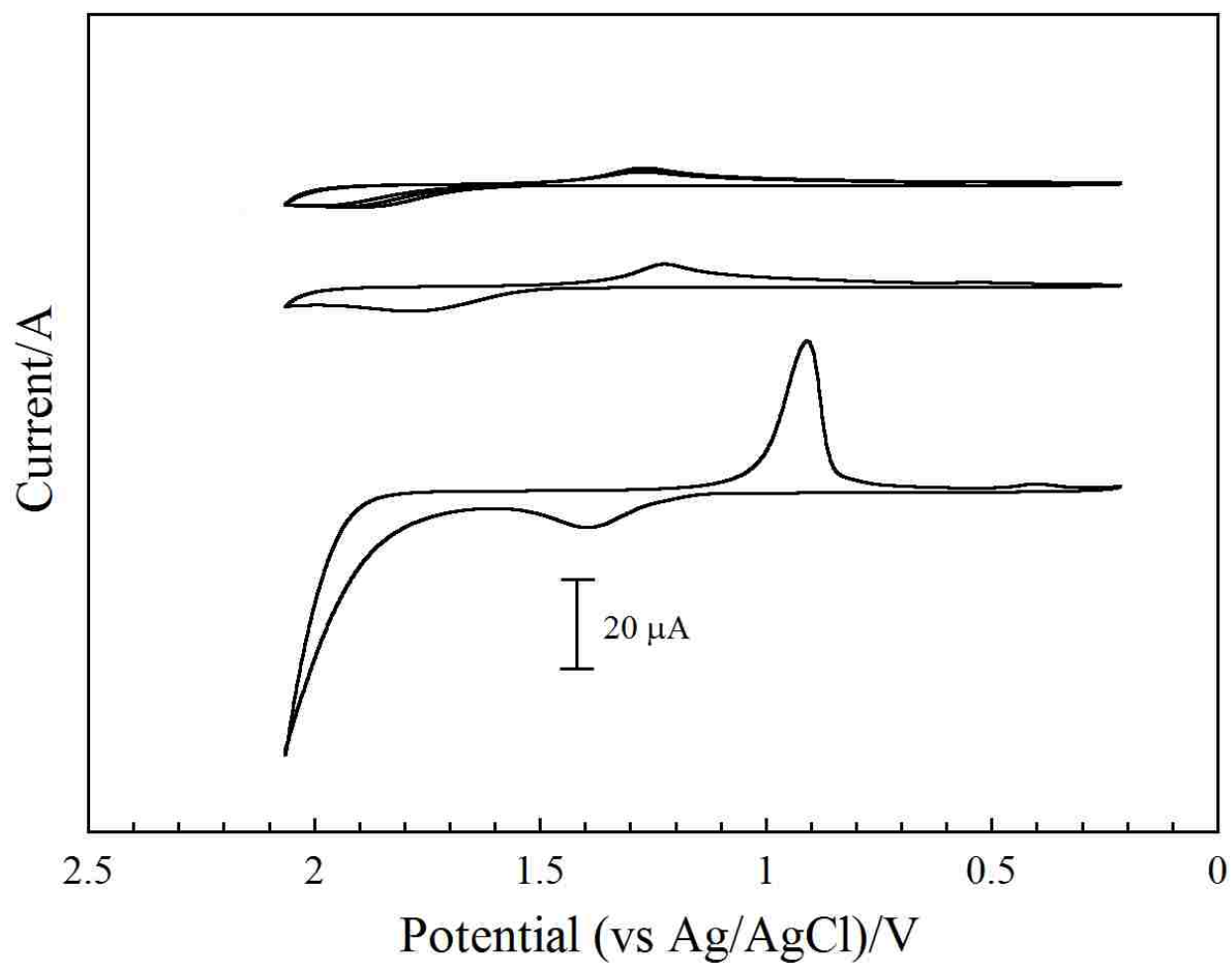


**Figure 9.** Top: IL purged with dry N<sub>2</sub> gas for 4, 6, and 12 hours. Middle: Pristine IL out of the bottle. Bottom: IL saturated with H<sub>2</sub>O.<sup>49</sup>

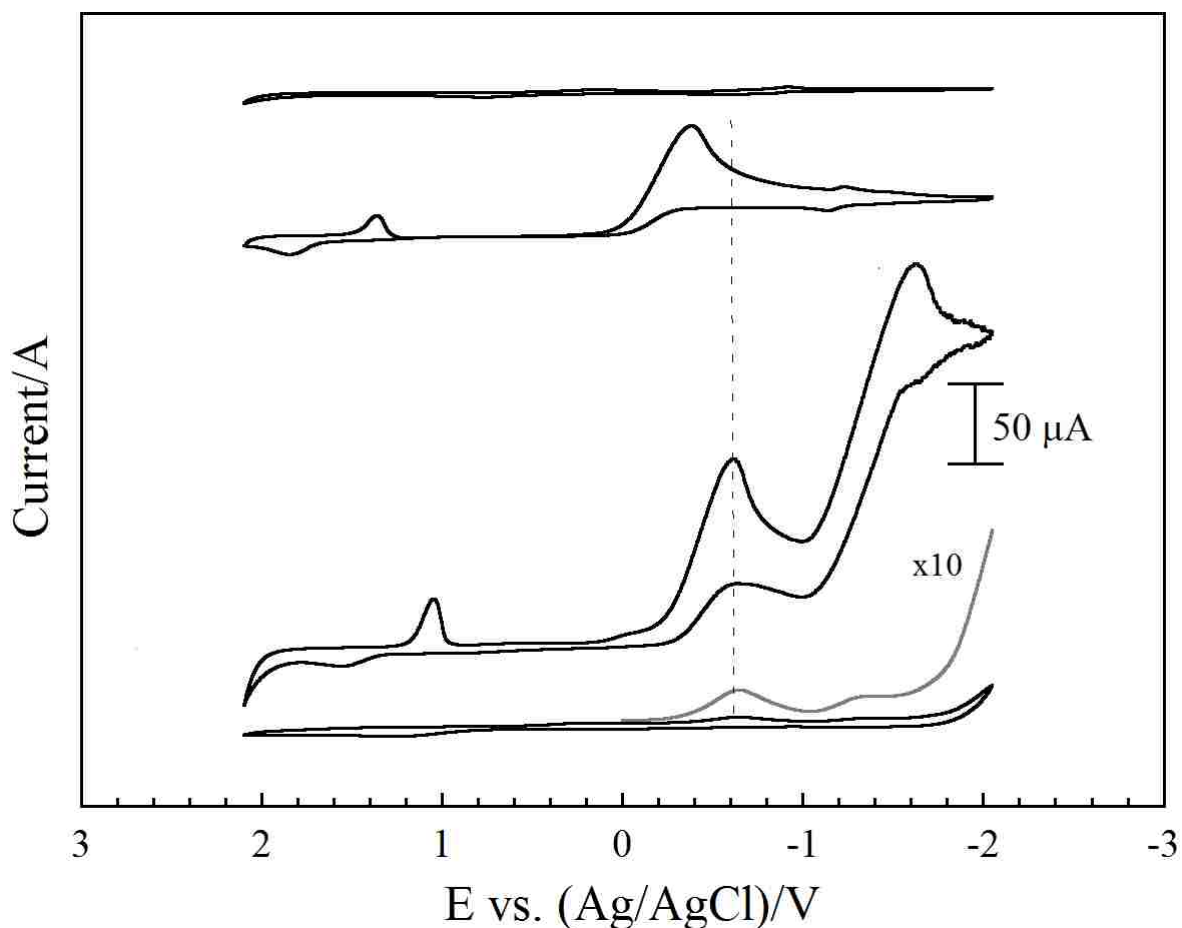


**Figure 10.** From top to bottom: Cyclic voltammetric responses on Au disc electrode of Dried IL, IL saturated with  $\text{H}_2\text{O}$ , IL saturated with  $\text{H}_2\text{O}$  and 0.5 M  $\text{HTf}_2\text{N}$ , and IL after  $\text{H}_2\text{O}$  removal and  $\text{HTf}_2\text{N}$  neutralization (as well as an enlarged version of the reduction scan).

The addition of  $\text{H}_2\text{O}$  into IL shows  $\text{H}^+$  adsorption around -0.4 V (**Figure 10**—2<sup>nd</sup> CV from the top). However, upon addition of 0.5 M  $\text{HTf}_2\text{N}$ , the  $\text{H}^+$  adsorption shifted to around -0.6 V and showed hydrogen evolution around -1.6 V. As the scan proceeded to more negative potential, the bubbles formed by the  $\text{H}_2$  evolution began to dominate the scan, causing the irregular lines. Excess acid in IL solution will hinder lanthanide deposition in the more negative potential due to hydrogen bubbles formation. After acid neutralization and water removal, the IL solution was almost back to its pristine IL form. With a closer look, however, the reduction scan showed the  $\text{H}^+$  adsorption

still exists, but the signal from it is minimal enough to not hinder lanthanide metal deposition at more negative potentials.

The cyclic voltammetry was performed using a glassy carbon electrode in a 150 mM samarium concentration in  $[\text{Me}_3\text{N}^n\text{Bu}][\text{Tf}_2\text{N}]$  with 0.545 M  $\text{HTf}_2\text{N}$  and 150 mM europium concentration in  $[\text{Me}_3\text{N}^n\text{Bu}][\text{Tf}_2\text{N}]$  with 0.704 M  $\text{HTf}_2\text{N}$ . For comparison, plain IL,  $[\text{Me}_3\text{N}^n\text{Bu}][\text{Tf}_2\text{N}]$ , was used for background. The addition of the  $\text{HTf}_2\text{N}$  was to provide proton for carbonate dissolution while limiting the competing ligands that could form a complex with the soluble samarium and europium. However, since water and acid can reduce the potential window and cause side reactions in the electrochemical analysis of soluble lanthanide, both acid and water must be removed or reduced as much as possible. The  $\text{Tf}_2\text{N}$  ligand is sufficiently high,  $> 4 \text{ M}$ , that complex formation with water is minimized. Excess  $\text{HTf}_2\text{N}$  was removed via extraction method with ultra-pure water and the IL was dried to minimize hydrogen evolution. The resulting water solution has a pH of about five which was still slightly acidic. However, it was sufficiently closer to neutral when compared to the initial pH ( $\sim 1$ ) for the lanthanide dissolved directly into IL using excess  $\text{HTf}_2\text{N}$ . A rotary evaporator was utilized at  $50 \text{ }^\circ\text{C}$  and 25 mbar to remove any excess water from the IL after the neutralization step.

The voltammetric response for the background IL and the samarium dissolved in IL is presented in **Figure 11** for the first cycle. The background was characterized by a small voltammetric wave at  $\sim -1.5 \text{ V vs. Ag/Ag}^+$  for samarium and  $\sim -1.4 \text{ V vs. Ag/Ag}^+$  for europium. It is possible that the voltammetric wave is due to the reduction of  $\text{H}^+$  and production of hydrogen due to the very low concentration of water remaining in the IL. In fact, the same voltammetric wave is observed in the IL containing dissolved lanthanides. However, a second voltammetric



wave associated with the reduction of samarium at the electrode is observed at  $\sim -1.9$  V vs. Ag/Ag<sup>+</sup> for samarium and  $\sim -2.1$  V vs. Ag/Ag<sup>+</sup> for europium.

Normally, the reduction of samarium and europium occurs through a two-step process from 3+ to 2+, followed by the reduction from 2+ to 0. Although there is an overlap between the lanthanide solutions and the IL background, the reduction is clearly resolved for the lanthanide metal depositions. In addition, the reduction of samarium at more negative potentials was observed in the large current increase between -2.4 V and -3.1 V. The reduction of europium was observed between -2.0 V through -3.1 V. In addition, the current associated with the processes are indicative of increased surface area of samarium deposits, as well as europium deposits. Both the first and final scans showed a decrease in current density as the scans are ran, which suggests that lanthanide species were deposited on the surface of the glassy carbon electrode. The voltammetry reaches a steady state with each sequential scan which shows that the glassy carbon surface has been modified due to surface adsorption. A bulk reduction of samarium occurs at potential more negative of -2.6 V which can be utilized in the bulk reduction and recovery of samarium metal. For europium, bulk reduction occurs at potential that is more negative of -2.4 V.

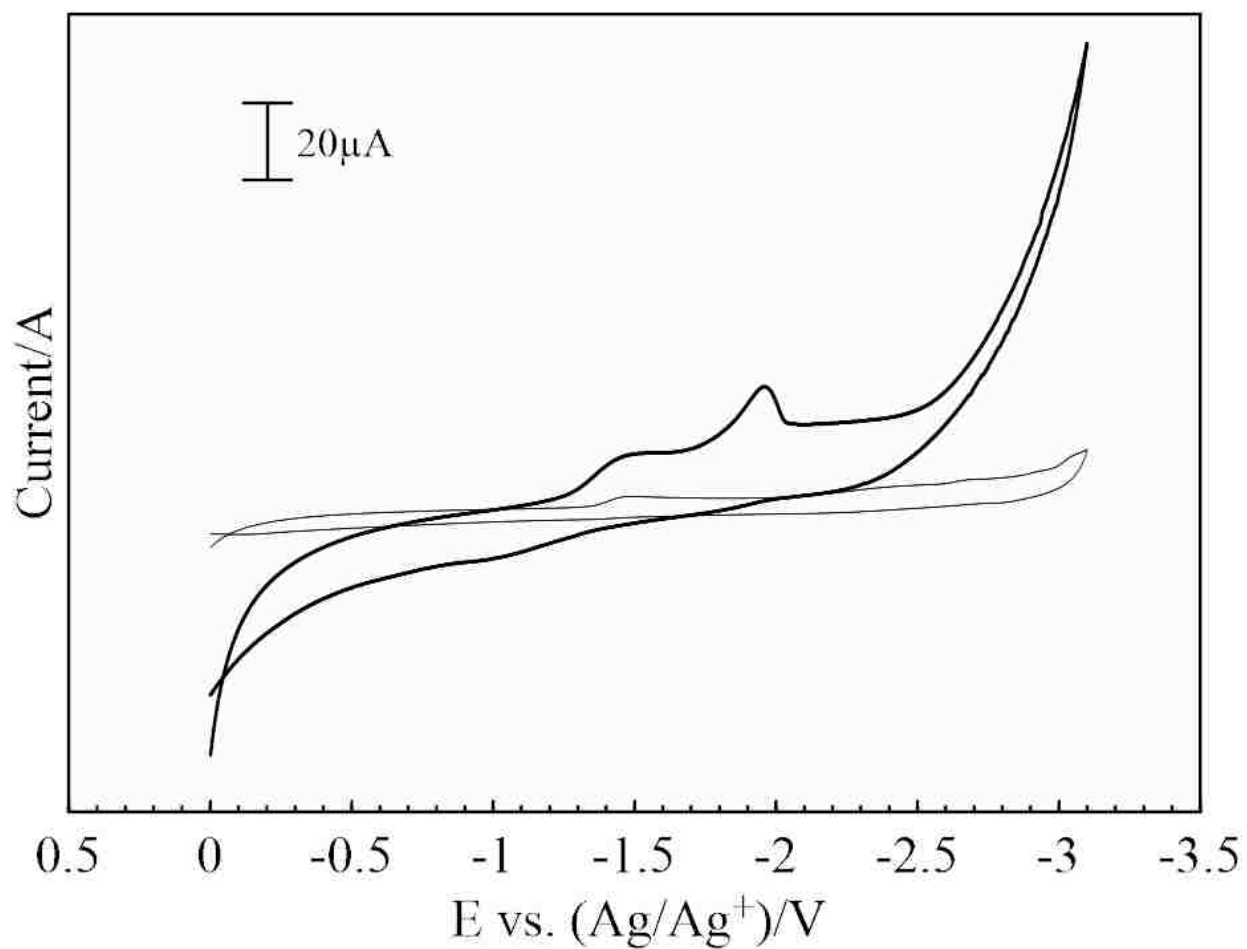


**Figure 11.** Cyclic voltammetry of the background IL (grey) and 150 mM samarium dissolved in IL (first cycle).

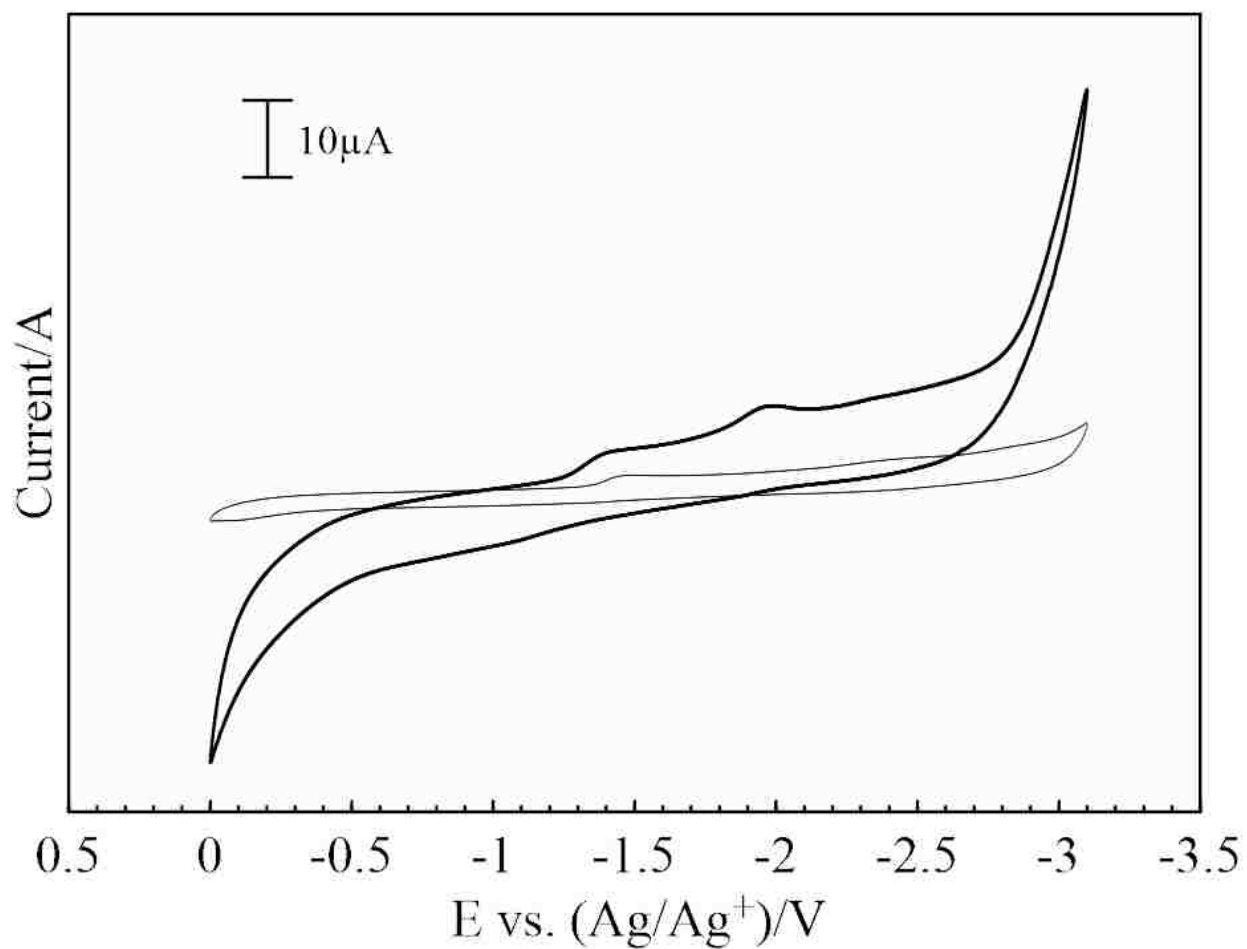


**Figure 12.** Cyclic voltammetry of the background IL (grey) and 150 mM samarium dissolved in IL (20 cycles).

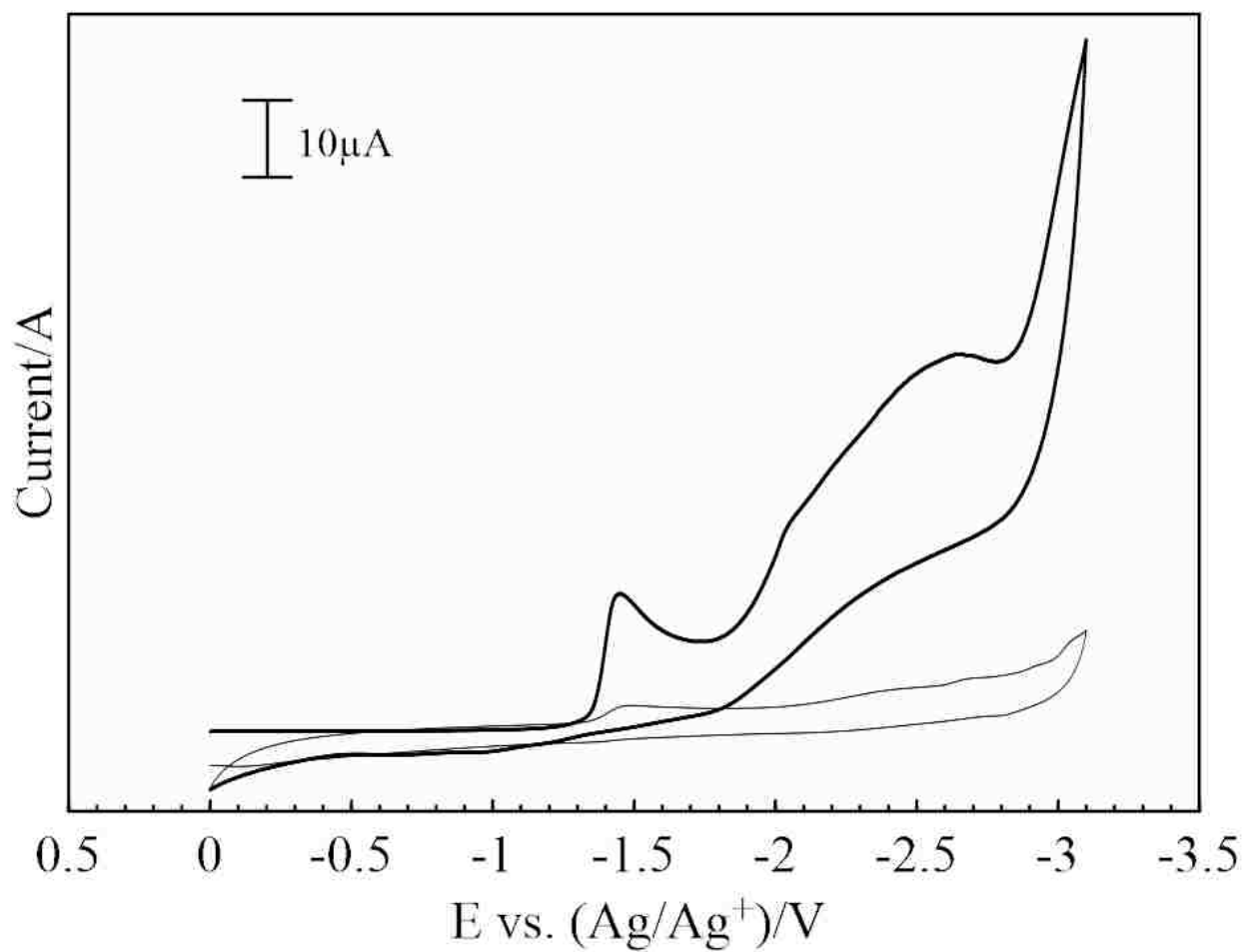


**Figure 13.** Cyclic voltammetry of the background IL (grey) and 150 mM europium dissolved in IL (first cycle).

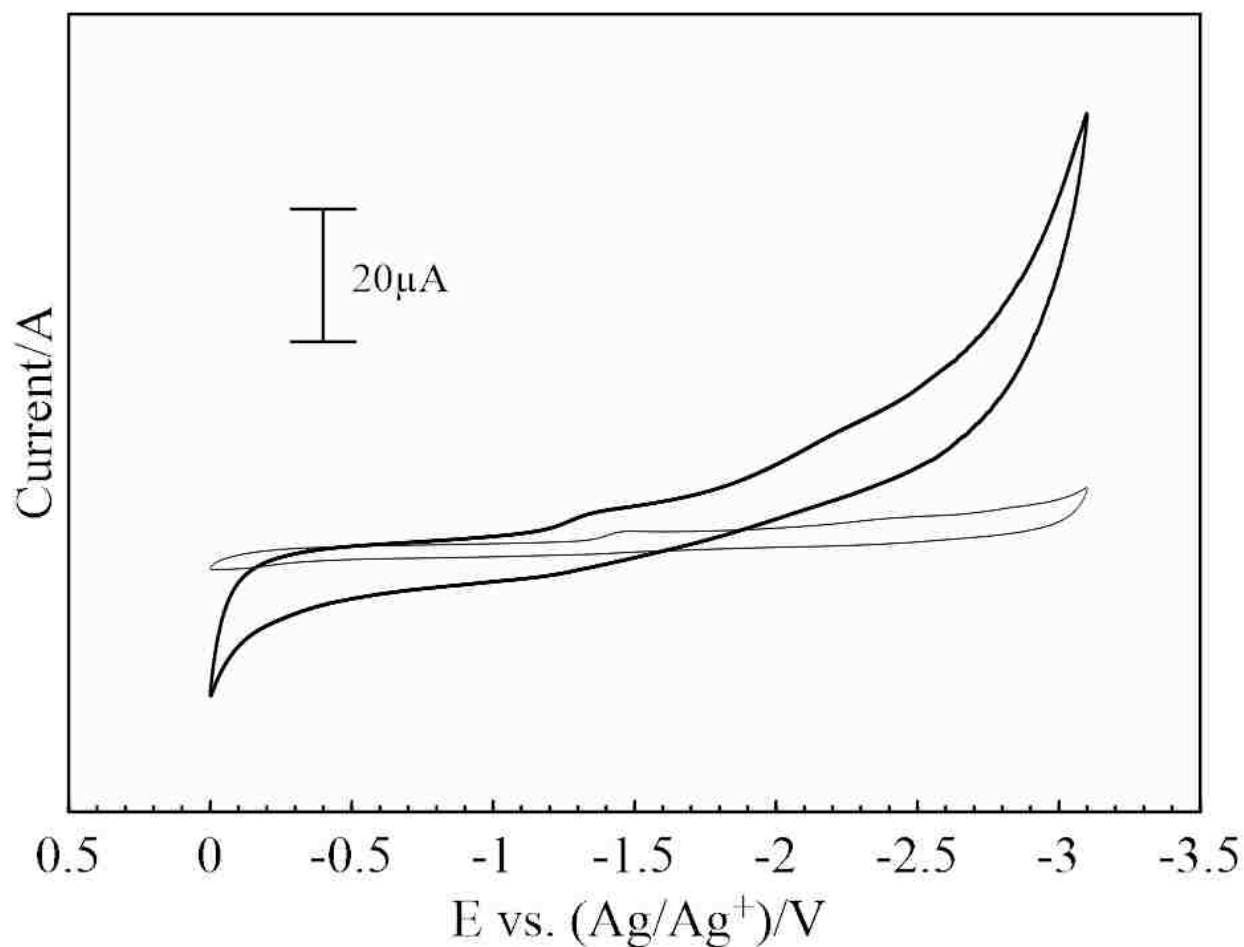


**Figure 14.** Cyclic voltammetry of the background IL (grey) and 150 mM europium dissolved in IL (20 cycles).

The anodic scans show the irreversibility of the adsorption on the glassy carbon electrode. There is no oxidation wave, which shows that desorption of samarium and europium species were kinetically hindered for this system. The lack of oxidation peak suggests that lanthanide deposits may be resistant to dissolution once deposited on the glassy carbon electrode.

### 3.3.2 Samarium and Europium Deposition on Grafoil

The glassy carbon disc electrode does not allow the lanthanide deposits to be evaluated with SEM. Therefore, a flat grafoil electrode was used to obtain the lanthanide deposits using similar conditions. The solution parameters were the same used in the cyclic voltammetry using glassy

carbon electrode. Initially, the grafoil electrode was subjected to twenty full scans using cyclic voltammetry to initiate lanthanide nucleation. After the nucleation sites were formed, amperometric deposition was run for 24 hours at -2.6 V for samarium and -2.4 V for europium to form thicker metal deposits. The solution needs to not be disturbed or stirred in order to keep the metal on the electrode. If stirring were to occur, some of the metal deposits will flake off of the grafoil. The deposit was carefully rinsed with ethanol, in order to wash off any excess IL and utilized for SEM analysis.

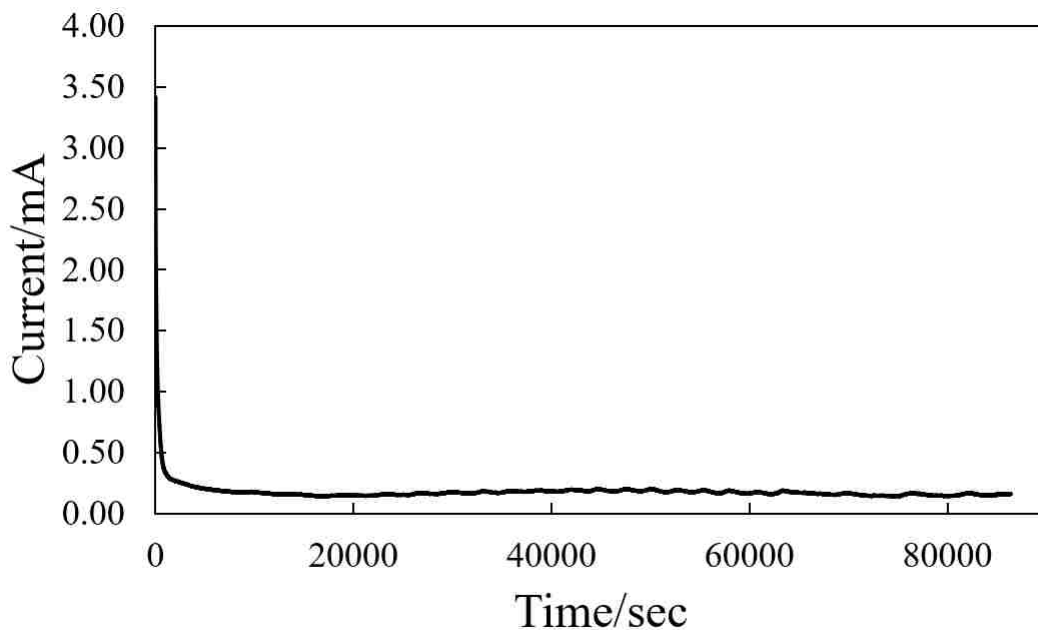


**Figure 15.** Amperometric deposition of 150 mM samarium in IL with HTf<sub>2</sub>N held at -2.6 V for 24 hours.

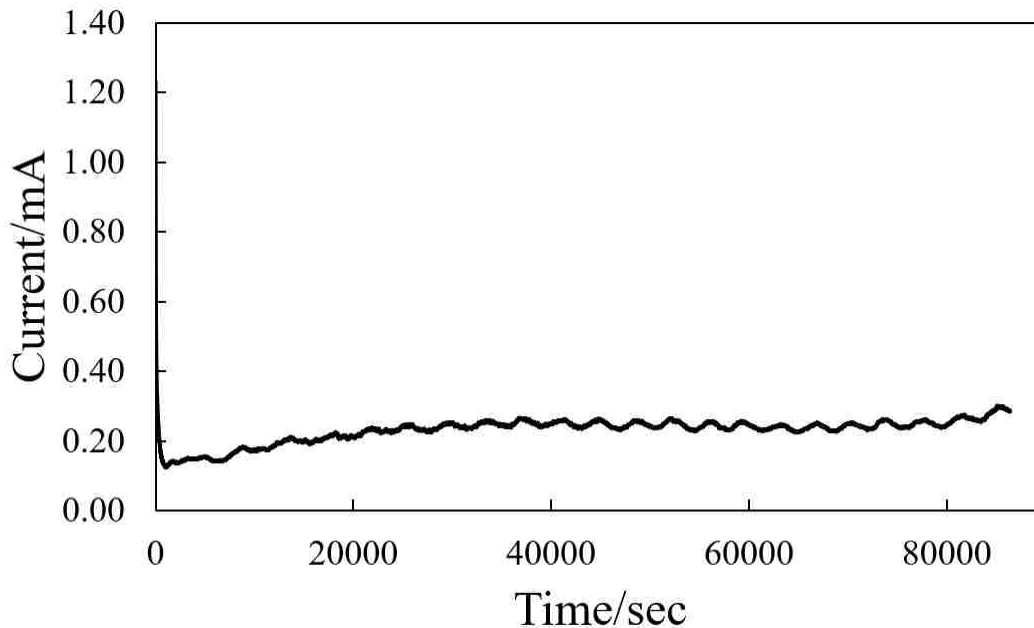


**Figure 16.** Amperometric deposition of 150 mM europium in IL with HTf<sub>2</sub>N held at -2.4 V for 24 hours.

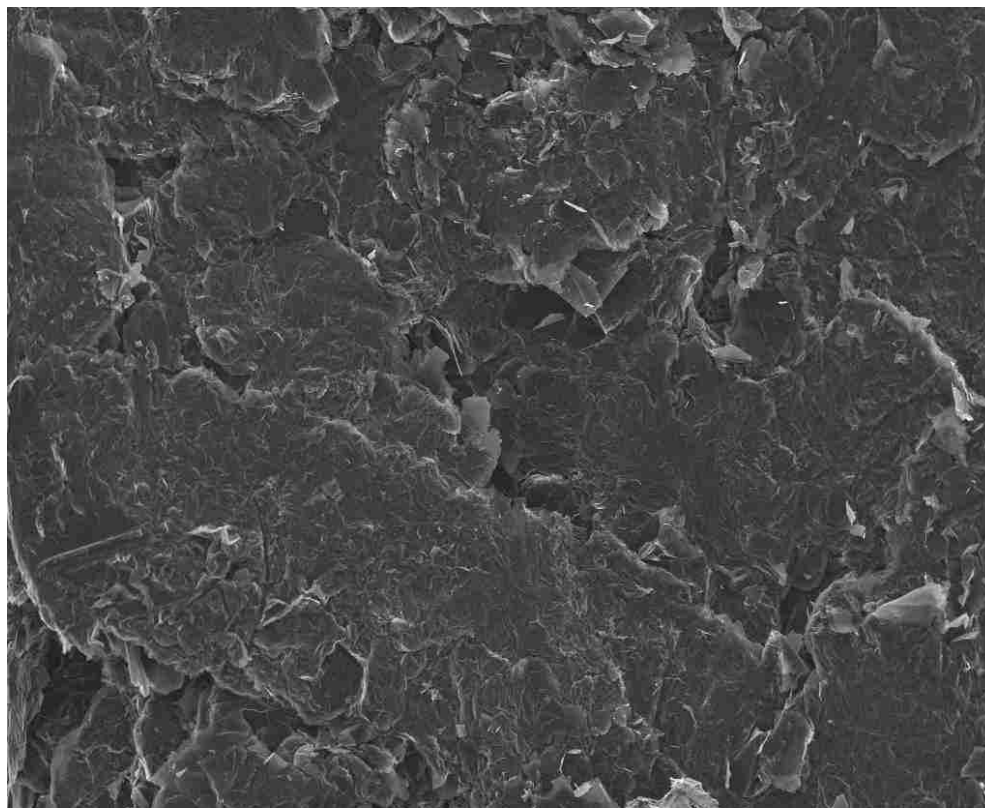
### 3.4 SEM/EDX

Cyclic voltammetry alone cannot verify the deposition of the lanthanide metals on the electrode. The deposits acquired through electrochemistry were further investigated through the use of JEOL-5610 scanning electron microscope equipped with a secondary electron and backscatter electron detectors. The elemental analysis was done through the use of the INCA mapping software connected to the SEM.

#### 3.4.1 SEM/EDX of the electrodeposition

Electrochemistry of plain IL on grafoil electrode was used as background in SEM/EDX. There was no preconditioning needed for the grafoil electrode used, but extra care was taken when using the grafoil electrode as any bend or fold in the electrode will cause it to crack and break. The strong carbon signal was expected to come from the grafoil. However, oxygen, fluoride, and sulfur bands also appeared on the background spectra and can be attributed to the Tf<sub>2</sub>N ligand due to IL not

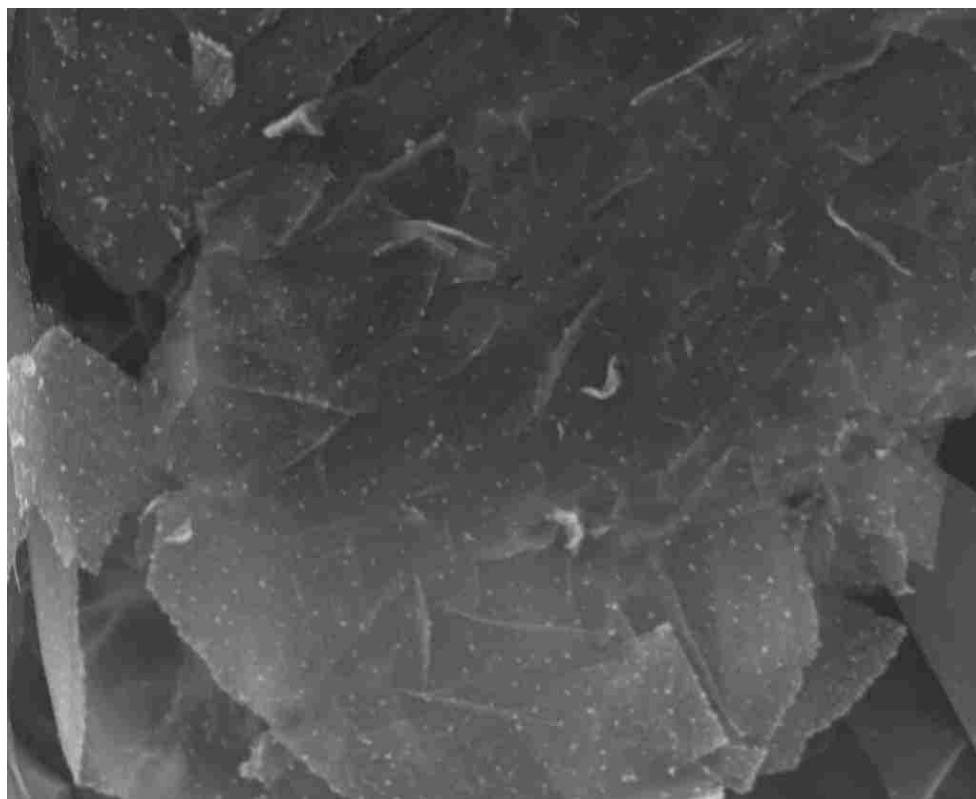
being fully washed off with ethanol. The flaky morphology of the grafoil can be attributed to its thinness. The grafoil loses its integrity the longer it is submerged in the IL solution. The weakened grafoil will no longer appear to be a smooth sheet, but rather scaly.



400 $\mu$ m

**Figure 17.** Grafoil 100x under SEM used for background IL.





20 $\mu$ m  
**Figure 18.** Grafoil 2000x under SEM used for background IL.

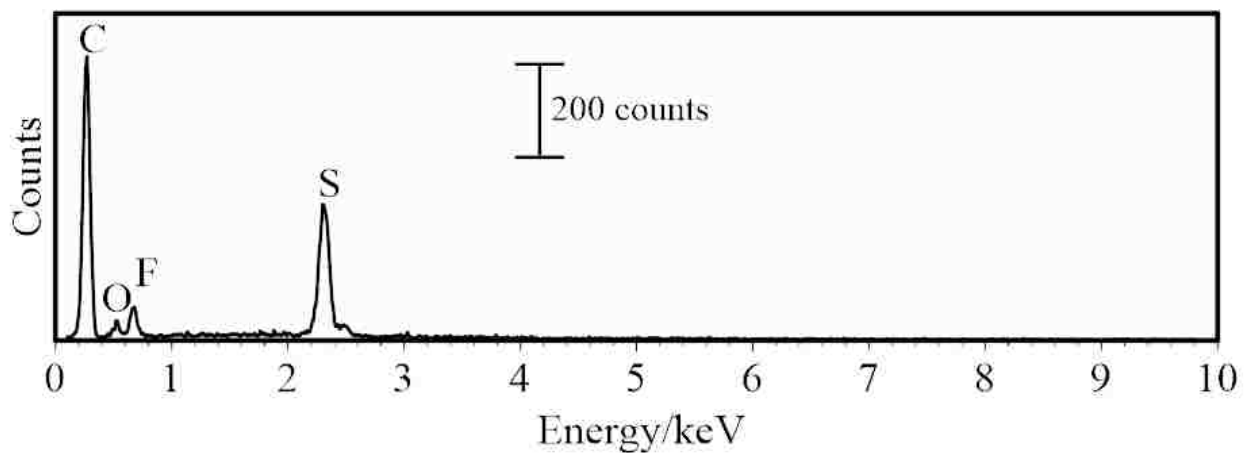


**Figure 19.** Grafoil 2000x EDX after exposure to IL without washing.

The deposited samarium on the grafoil electrode shows a metallic sheen indicating that the surface was coated with samarium metal. The dark areas in the SEM represent the grafoil electrode

where samarium nucleation sites did not form. The flakiness of the grafoil electrode caused the samarium nucleation sites to congregate into chunks, preventing the samarium from coalescing. The 2000x magnification shows a crack where the grafoil electrode started to lose its integrity.

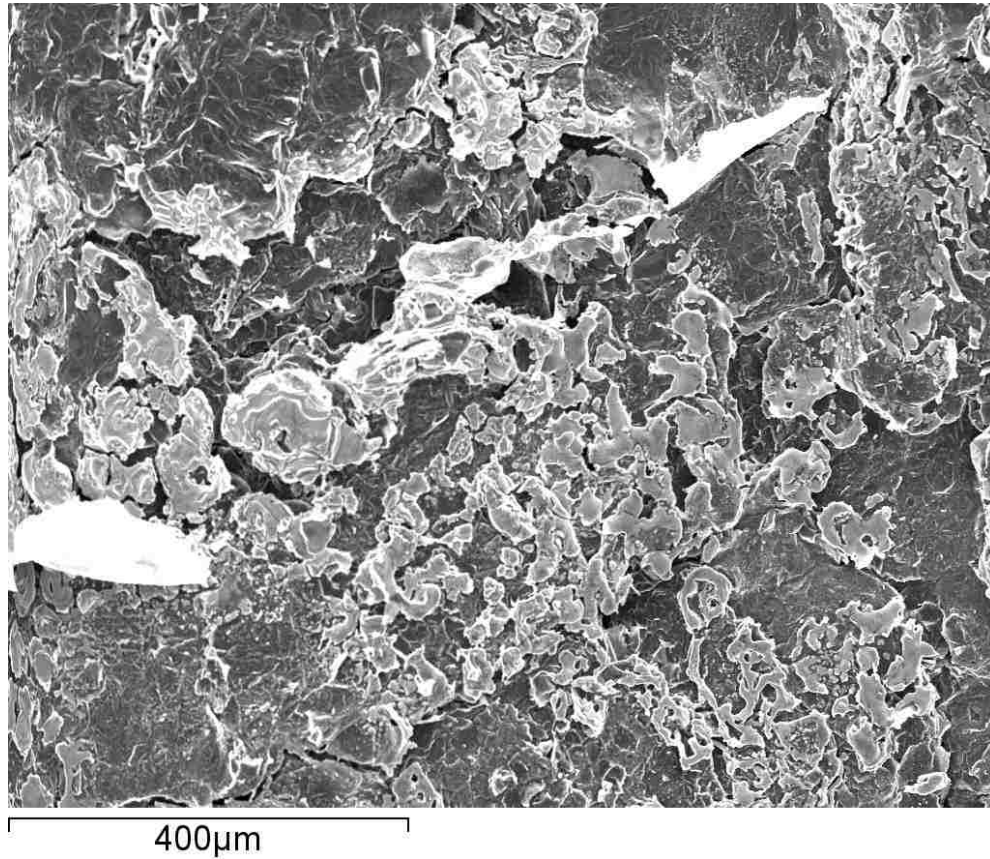
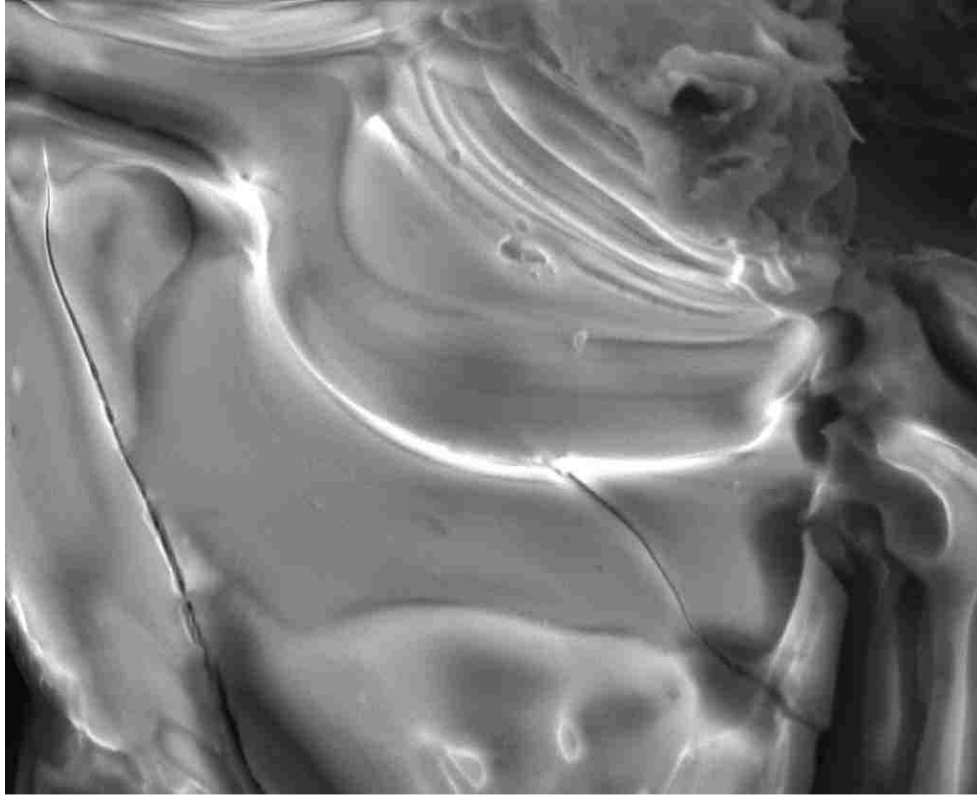


**Figure 20.** SEM of Samarium deposits at 100x magnification.



20 $\mu$ m  
**Figure 21.** SEM of Samarium deposits at 2000x magnification.

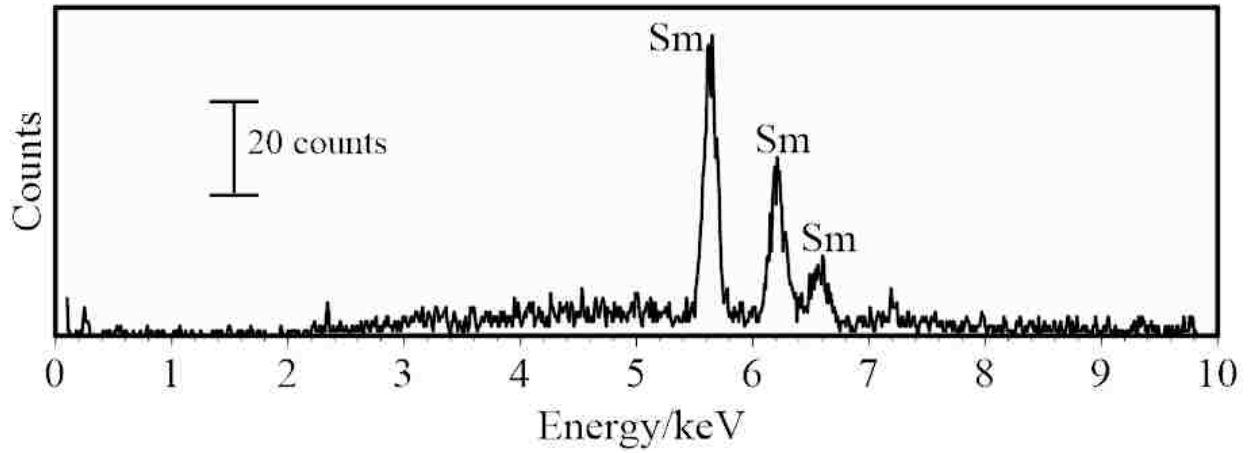
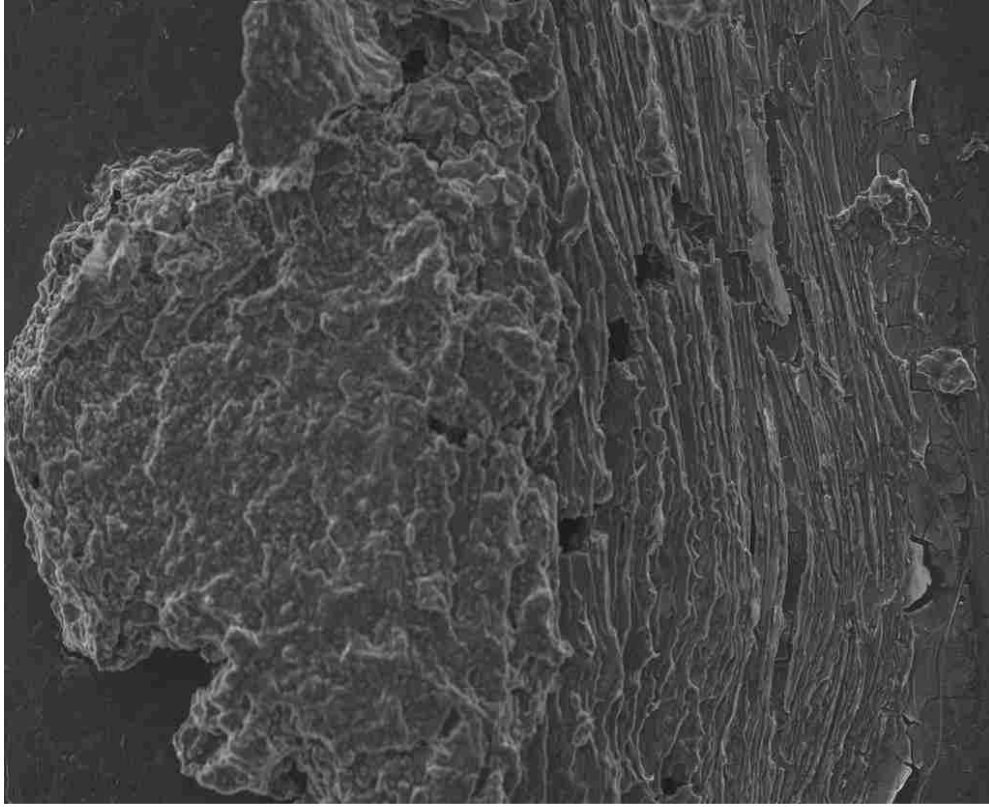


**Figure 22.** Samarium metal 2000x EDX.

Characteristic X-rays are caused by the transition of electrons between inner orbits. The inner orbits are typically full of electrons. In EDX, the sample is bombarded with electrons, causing a vacancy in the inner orbit. These X-ray photon energies are specific to each element.<sup>50</sup>

Literature reports emission signals for samarium to be  $L\alpha_1$  5.633 keV,  $L\beta_1$  6.201 keV, and  $L\gamma_1$  6.717 keV.<sup>50-52</sup> The experimental emissions signal with samarium are 5.636 keV, 6.205 keV, and 6.587 keV. These values are consistent with the values reported in literature and are, therefore, indicative of a successful samarium deposition on the grafoil electrode. The SEM/EDX results confirm that the surface deposition of samarium species from direct dissolution of  $\text{Sm}_2(\text{CO}_3)_3 \cdot x\text{H}_2\text{O}$  is achieved electrochemically. The SEM for the europium deposit on grafoil electrode shows europium coalesced from its nucleation site. The nonmetallic appearance can be attributed to remnants of IL that were not fully washed off the surface of the grafoil electrode with ethanol. The flaky appearance of the deposit can be attributed to the cracking of the grafoil electrode upon which it was deposited. The darker areas around the edges represents the grafoil electrode where europium nucleation sites did not form.



400 $\mu$ m  
**Figure 23.** SEM of Europium deposits at 100x magnification.

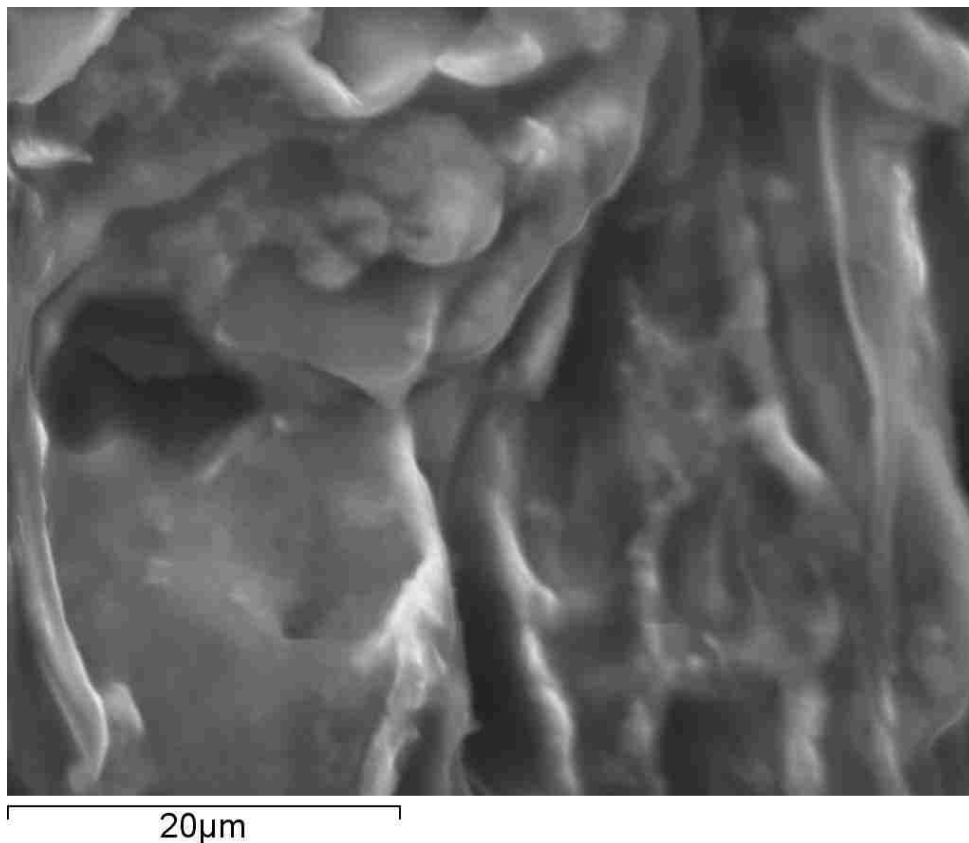


**Figure 24.** SEM of Europium deposits at 2000x magnification.

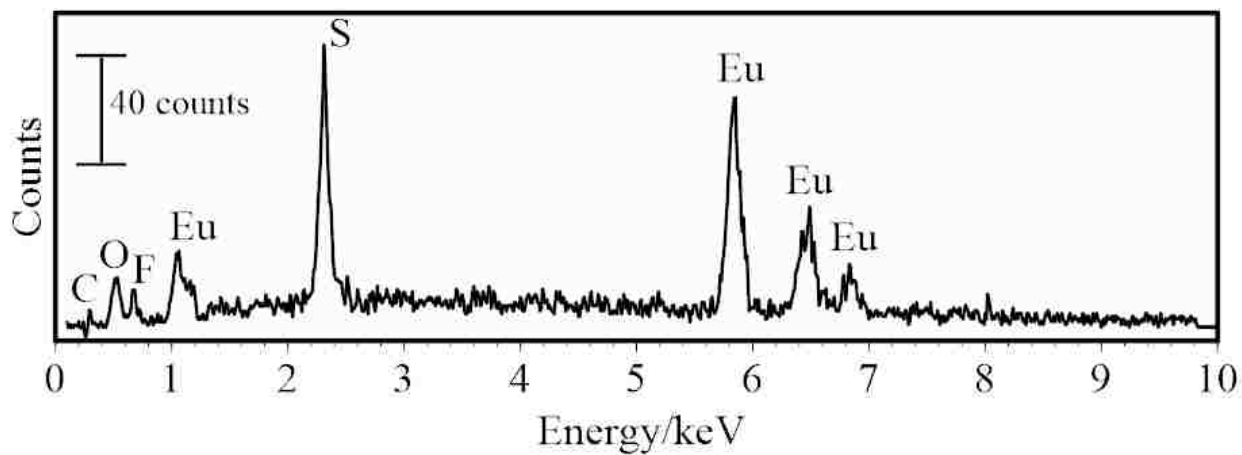


**Figure 25.** Europium metal 2000x EDX.

Literature for europium reports emission signals to be  $M\alpha_1$  1.131 keV,  $L\alpha_1$  5.849 keV,  $L\beta_1$  6.458 keV, and  $L\gamma_1$  6.977 keV. The corresponding signal with europium are 1.131 keV, 5.815 keV,

6.456 keV, and 6.841 keV, and therefore is indicative of a successful europium deposition on the grafoil electrode. Residual  $\text{Tf}_2\text{N}$  can be found on the EDX which could be removed by rinsing the grafoil again with ethanol. The SEM/EDX results confirm that the surface deposition of europium species from direct dissolution of  $\text{Eu}_2(\text{CO}_3)_3 \cdot x\text{H}_2\text{O}$  is achieved electrochemically.

### 3.5 Conclusion

The direct dissolution of  $\text{Sm}_2(\text{CO}_3)_3 \cdot x\text{H}_2\text{O}$  and  $\text{Eu}_2(\text{CO}_3)_3 \cdot x\text{H}_2\text{O}$  in IL with  $\text{HTf}_2\text{N}$  was demonstrated. The formation and decomposition of carbonic acid aided with the direct dissolution of the lanthanide species. The addition of the  $\text{HTf}_2\text{N}$  avoided the introduction of competing species in the solution promoting coordination between samarium and  $\text{Tf}_2\text{N}$  ligand and between the europium and  $\text{Tf}_2\text{N}$  ligand. The UV-Vis showed electronic transitions that are associated with the f-element electronic transitions associated with the formation of samarium and  $\text{Tf}_2\text{N}$  complexes, as well as the europium and the  $\text{Tf}_2\text{N}$  complexes. Fine structures are indicative of multiple electronic transitions that are associated with soluble samarium and soluble europium. The electrochemical analysis was performed using glassy carbon electrode. The peaks shown by the voltammetry indicates the deposition of samarium and europium as they proceeded through the loss of  $\text{Tf}_2\text{N}$  ligand at the electrode surface. A 24-hour deposition of the lanthanides in a grafoil electrode was utilized in order to verify deposition on the electrode. SEM/EDX analysis was used to visualize and confirm the deposition. The results confirm that  $\text{Sm}_2(\text{CO}_3)_3 \cdot x\text{H}_2\text{O}$  and  $\text{Eu}_2(\text{CO}_3)_3 \cdot x\text{H}_2\text{O}$  in IL with  $\text{HTf}_2\text{N}$  can be reclaimed through electrochemical means in the form of metal deposits.

## Chapter 4. Conclusion

This thesis examined the hypothesis that the direct dissolution of Sm and Eu carbonates could be achieved in IL solutions producing soluble metal species at sufficient concentrations to facilitate the electrochemical recovery of metal. The advantage of using these ILs was demonstrated with electrochemical potential windows greater than 3 V that extend to sufficiently negative values to facilitate the deposition of the electropositive lanthanide metal species. The direct dissolution of  $\text{Sm}_2(\text{CO}_3)_3 \cdot x\text{H}_2\text{O}$  and  $\text{Eu}_2(\text{CO}_3)_3 \cdot x\text{H}_2\text{O}$  into protic IL,  $[\text{Me}_3\text{N}^n\text{Bu}][\text{Tf}_2\text{N}]$ , containing the conjugate acid,  $\text{HTf}_2\text{N}$ , was demonstrated. The direct dissolution is accomplished through the evolution and decomposition of carbonic acid following degassing to remove  $\text{CO}_2$  and water from the IL. This approach minimized the inclusion of additional chemical species in the IL to promote coordination between soluble Sm and Eu and the  $\text{Tf}_2\text{N}$  ligand. The addition of water and  $\text{HTf}_2\text{N}$  allowed for the direct dissolution to be achieved by creating solvation spheres from water and helped to facilitate the interaction between the  $\text{HTf}_2\text{N}$ , the lanthanide carbonates, and the IL. The direct dissolution of Sm and Eu carbonates produced soluble chemical species in IL solutions at sufficient concentrations to facilitate the electrochemical recovery of the metals. Even though water and  $\text{HTf}_2\text{N}$  were necessary for the dissolution of the lanthanide species, their removal was vital for the electrochemical deposition on the working electrode. Electrochemical analysis of soluble Sm and Eu in  $[\text{Me}_3\text{N}^n\text{Bu}][\text{Tf}_2\text{N}]$  was performed with a glassy carbon electrode. The multi-wave voltammetry observed suggests that the deposition of Sm and Eu species proceeds through and reductive loss of  $\text{Tf}_2\text{N}$  at the electrode surface. The deposition of Sm and Eu species on grafoil was confirmed using SEM with EDX analysis. The only known metal deposition for samarium from IL was achieved. The results for Sm and Eu suggests that the protic ILs can be used to enhance the solubility of other trivalent lanthanide carbonate species through direct dissolution.



## References

1. Walden, P., Molecular weights and electrical conductivity of several fused salts. *Bull. Acad. Imp. Sci. St.-Petersbourg* **1914**, 405-22.
2. Armand, M.; Endres, F.; MacFarlane, D. R.; Ohno, H.; Scrosati, B., Ionic-liquid materials for the electrochemical challenges of the future. *Nat. Mater.* **2009**, 8, 621-629.
3. Belieres, J.-P.; Angell, C. A., Protic ionic liquids: preparation, characterization, and proton free energy level representation. *J. Phys. Chem. B* **2007**, 111, 4926-4937.
4. Singh, V. V.; Nigam, A. K.; Batra, A.; Boopathi, M.; Singh, B.; Vijayaraghavan, R., Applications of ionic liquids in electrochemical sensors and biosensors. *Int. J. Electrochem.* **2012**, 165683, 19 pp.
5. Wier, T. P. The electrodeposition of metals in fused quaternary ammonium salts. Rice University, 1942.
6. Hurley, F. H.; Wier, T. P., Jr., Electrodeposition of metals from fused quaternary ammonium salts. *J. Electrochem. Soc.* **1951**, 98, 203-6.
7. Wilkes, J. S.; Zaworotko, M. J., AIR AND WATER STABLE 1-ETHYL-3-METHYLIMIDAZOLIUM BASED IONIC LIQUIDS. *J. Chem. Soc.-Chem. Commun.* **1992**, 965-967.
8. Bonhote, P.; Dias, A.-P.; Papageorgiou, N.; Kalyanasundaram, K.; Grätzel, M., Hydrophobic, highly conductive ambient-temperature molten salts. *Inorg. Chem.* **1996**, 35, 1168-1178.
9. O'Mahony, A. M.; Silvester, D. S.; Aldous, L.; Hardacre, C.; Compton, R. G., Effect of water on the electrochemical window and potential limits of room-temperature ionic liquids. *Journal of Chemical & Engineering Data* **2008**, 53, 2884-2891.
10. Galiński, M.; Lewandowski, A.; Stepniak, I., Ionic liquids as electrolytes. *Electrochimica Acta* **2006**, 51, 5567-5580.
11. Cammarata, L.; Kazarian, S. G.; Salter, P. A.; Welton, T., Molecular states of water in room temperature ionic liquids. *Phys. Chem. Chem. Phys.* **2001**, 3, 5192-5200.
12. Feng, G.; Jiang, X. K.; Qiao, R.; Kornyshev, A. A., Water in Ionic Liquids at Electrified Interfaces: The Anatomy of Electrosorption. *ACS Nano* **2014**, 8, 11685-11694.
13. Lide, D. R., *CRC Handbook of Chemistry and Physics*. 85th ed.; CRC Press: 2004.
14. Rendall, J. S.; Vaughn, V. W., Jr. Method for extraction of valuable minerals and precious metals from oil sands ore bodies and other related ore bodies. CA2044731A1, 1991.
15. Endres, F.; El Abedin, S. Z.; Saad, A. Y.; Moustafa, E. M.; Borissenko, N.; Price, W. E.; Wallace, G. G.; MacFarlane, D. R.; Newman, P. J.; Bund, A., On the electrodeposition of titanium in ionic liquids. *Phys. Chem. Chem. Phys.* **2008**, 10, 2189-2199.
16. Aldous, L.; Silvester, D. S.; Pitner, W. R.; Compton, R. G.; Lagunas, M. C.; Hardacre, C., Voltammetric studies of gold, protons, and [HCl<sub>2</sub>]<sup>-</sup> in ionic liquids. *The Journal of Physical Chemistry C* **2007**, 111, 8496-8503.
17. Al-Salman, R.; El Abedin, S. Z.; Endres, F., Electrodeposition of Ge, Si and Si x Ge 1- x from an air-and water-stable ionic liquid. *Phys. Chem. Chem. Phys.* **2008**, 10, 4650-4657.
18. Binnemans, K., Lanthanides and actinides in ionic liquids. *Chemical reviews* **2007**, 107, 2592-2614.
19. Lohrengel, M. M.; Schultze, J. W., ELECTROCHEMICAL PROPERTIES OF ANODIC GOLD OXIDE LAYERS .1. POTENTIOSTATIC OXIDE-GROWTH AND DOUBLE-LAYER CAPACITY. *Electrochimica Acta* **1976**, 21, 957-965.

20. Bhatt, A. I.; Duffy, N. W.; Collison, D.; May, I.; Lewin, R. G., Cyclic Voltammetry of Th (IV) in the Room-Temperature Ionic Liquid [Me<sub>3</sub>N n Bu][N (SO<sub>2</sub>CF<sub>3</sub>)<sub>2</sub>]. *Inorg. Chem.* **2006**, 45, 1677-1682.
21. Bhatt, A. I.; May, I.; Volkovich, V. A.; Collison, D.; Helliwell, M.; Polovov, I. B.; Lewin, R. G., Structural characterization of a lanthanum bistriflimide complex, La(N(SO<sub>2</sub>CF<sub>3</sub>)(2))(3)(H<sub>2</sub>O)(3), and an investigation of La, Sm, and Eu electrochemistry in a room-temperature ionic liquid, (Me<sub>3</sub>NBu)-Bu-n N(SO<sub>2</sub>CF<sub>3</sub>)(2). *Inorg. Chem.* **2005**, 44, 4934-4940.
22. Legeai, S.; Diliberto, S.; Stein, N.; Boulanger, C.; Estager, J.; Papaiconomou, N.; Draye, M., Room-temperature ionic liquid for lanthanum electrodeposition. *Electrochem. Commun.* **2008**, 10, 1661-1664.
23. Nockemann, P.; Thijs, B.; Pittois, S.; Thoen, J.; Glorieux, C.; Van Hecke, K.; Van Meervelt, L.; Kirchner, B.; Binnemans, K., Task-specific ionic liquid for solubilizing metal oxides. *The Journal of Physical Chemistry B* **2006**, 110, 20978-20992.
24. Branco, L. C.; Rosa, J. N.; Moura Ramos, J. J.; Afonso, C. A., Preparation and characterization of new room temperature ionic liquids. *Chemistry—A European Journal* **2002**, 8, 3671-3677.
25. Yamagata, M.; Katayama, Y.; Miura, T., Electrochemical behavior of samarium, europium, and ytterbium in hydrophobic room-temperature molten salt systems. *Journal of the Electrochemical Society* **2006**, 153, E5-E9.
26. Aono, M.; Imai, Y.; Abe, H.; Matsumoto, H.; Yoshimura, Y., UV-vis spectroscopic study of room temperature ionic liquid-water mixtures: N,N-diethyl-N-methyl-N-(2-methoxyethyl) ammonium tetrafluoroborate. *Thermochim. Acta* **2012**, 532, 179-182.
27. Pan, Y.; Hussey, C. L., Electrochemical and Spectroscopic Investigation of Ln<sup>3+</sup> (Ln = Sm, Eu, and Yb) Solvation in Bis(trifluoromethylsulfonyl)imide-Based Ionic Liquids and Coordination by N,N,N',N'-Tetraoctyl-3-oxa-pentane Diamide (TODGA) and Chloride. *Inorg. Chem.* **2013**, 52, 3241-3252.
28. Nockemann, P.; Servaes, K.; Van Deun, R.; Van Hecke, K.; Van Meervelt, L.; Binnemans, K.; Görrler-Walrand, C., Speciation of uranyl complexes in ionic liquids by optical spectroscopy. *Inorg. Chem.* **2007**, 46, 11335-11344.
29. Binnemans, K.; Jones, P. T.; Blanpain, B.; Van Gerven, T.; Yang, Y.; Walton, A.; Buchert, M., Recycling of rare earths: a critical review. *Journal of Cleaner Production* **2013**, 51, 1-22.
30. Wilkes, J. S.; Levisky, J. A.; Wilson, R. A.; Hussey, C. L., Dialkylimidazolium chloroaluminate melts: a new class of room-temperature ionic liquids for electrochemistry, spectroscopy and synthesis. *Inorg. Chem.* **1982**, 21, 1263-1264.
31. Robinson, J.; Osteryoung, R., An electrochemical and spectroscopic study of some aromatic hydrocarbons in the room temperature molten salt system aluminum chloride-n-butylpyridinium chloride. *Journal of the American Chemical Society* **1979**, 101, 323-327.
32. Lipsztajn, M.; Osteryoung, R. A., Electrochemistry in neutral ambient-temperature ionic liquids. 1. Studies of iron (III), neodymium (III), and lithium (I). *Inorg. Chem.* **1985**, 24, 716-719.
33. Billard, I.; Mekki, S.; Gaillard, C.; Hesemann, P.; Moutiers, G.; Mariet, C.; Labet, A.; Bünzli, J. C. G., Eu<sup>III</sup> luminescence in a hygroscopic ionic liquid: effect of water and evidence for a complexation process. *European Journal of Inorganic Chemistry* **2004**, 2004, 1190-1197.
34. Swatloski, R. P.; Holbrey, J. D.; Rogers, R. D., Ionic liquids are not always green: hydrolysis of 1-butyl-3-methylimidazolium hexafluorophosphate. *Green Chemistry* **2003**, 5, 361-363.

35. Douglas A. Skoog, F. J. H., Stanley R. Crouch, *Principles of Instrumental Analysis*. Thomson Brooks/Cole: 2007.
36. Bard, A. J.; Parsons, R.; Jordan, J., *Standard Potentials in Aqueous Solution*. Taylor & Francis: 1985.
37. Saheb, A.; Janata, J.; Josowicz, M., Reference electrode for ionic liquids (vol 18, pg 405, 2006). *Electroanalysis* **2007**, 19, 1222-1222.
38. Lunstroot, K.; Nockemann, P.; Van Hecke, K.; Van Meervelt, L.; Görller-Walrand, C.; Binnemans, K.; Driesen, K., Visible and near-infrared emission by samarium (III)-containing ionic liquid mixtures. *Inorg. Chem.* **2009**, 48, 3018-3026.
39. Viveros-Andrade, A. G.; Colorado-Peralta, R.; Flores-Alamo, M.; Castillo-Blum, S. E.; Durán-Hernández, J.; Rivera, J. M., Solvothermal synthesis and spectroscopic characterization of three lanthanide complexes with high luminescent properties [H<sub>2</sub>NMe<sub>2</sub>]<sub>3</sub>[Ln(III)(2,6-pyridinedicarboxylate)<sub>3</sub>] (Ln = Sm, Eu, Tb): In the presence of 4,4'-Bipyridyl. *Journal of Molecular Structure* **2017**, 1145, 10-17.
40. Peacock, R., Structure and bonding. *Berlin* **1975**, 22, 83.
41. Binnemans, K.; Görller-Walrand, C., Polarized absorption spectra of Eu(BrO<sub>3</sub>)<sub>3</sub>·9H<sub>2</sub>O. *Journal of Physics: Condensed Matter* **1996**, 8, 1267.
42. Banks, C. V.; Klingman, D. W., Spectrophotometric determination of rare earth mixtures. *Analytica Chimica Acta* **1956**, 15, 356-363.
43. Dyke, J.; Hush, N., A spectroscopic study of Eu (III)/Eu (II) and Sm (III)/Sm (II) solutions in acetonitrile obtained by controlled-potential reduction. *Journal of Electroanalytical Chemistry and Interfacial Electrochemistry* **1972**, 36, 337-347.
44. Butement, F., Absorption and fluorescence spectra of bivalent samarium, europium and ytterbium. *Transactions of the Faraday Society* **1948**, 44, 617-626.
45. Jiang, J.; Higashiyama, N.; Machida, K.-i.; Adachi, G.-y., The luminescent properties of divalent europium complexes of crown ethers and cryptands. *Coordination chemistry reviews* **1998**, 170, 1-29.
46. Higashiyama, N.; Takemura, K.; Kimura, K.; Adachi, G.-y., Luminescence of divalent europium complexes with N-pivot lariat azacrown ethers. *Inorganica chimica acta* **1992**, 194, 201-206.
47. Sabbatini, N.; Ciano, M.; Dellonte, S.; Bonazzi, A.; Balzani, V., Absorption and emission properties of a europium (II) cryptate in aqueous solution. *Chemical Physics Letters* **1982**, 90, 265-268.
48. Billard, I.; Moutiers, G.; Labet, A.; El Azzi, A.; Gaillard, C.; Mariet, C.; Lützenkirchen, K., Stability of divalent europium in an ionic liquid: Spectroscopic investigations in 1-methyl-3-butylimidazolium hexafluorophosphate. *Inorg. Chem.* **2003**, 42, 1726-1733.
49. Droessler, J. E.; Czerwinski, K. R.; Hatchett, D. W., Electrochemical Measurement of Gold Oxide Reduction and Methods for Acid Neutralization and Minimization of Water in Wet Ionic Liquid. *Electroanalysis* **2014**, 26, 2631-2638.
50. Introduction to Energy Dispersive X-ray Spectrometry (EDS).
51. Periodic Table of Elements and X-ray Energies. [https://www.bruker.com/fileadmin/user\\_upload/8-PDF-Docs/X-rayDiffraction\\_ElementalAnalysis/HH-XRF/Misc/Periodic Table and X-ray Energies.pdf](https://www.bruker.com/fileadmin/user_upload/8-PDF-Docs/X-rayDiffraction_ElementalAnalysis/HH-XRF/Misc/Periodic Table and X-ray Energies.pdf)
52. Your Periodic Table. <http://www.yourperiodictable.com/>

## Curriculum Vitae

### **Eden Beatriz Martinez**

4505 S. Maryland Parkway  
Department of Chemistry and Biochemistry  
University of Nevada, Las Vegas  
Las Vegas, NV 89154  
Office Phone: (702)895-2658  
E-mail address: bea.martinez2424@gmail.com

#### Education

University of Nevada, Las Vegas  
B.S., Biochemistry, May 2011

The Electrochemical Deposition of Samarium and Europium Dissolved in Ionic Liquid Solvent

Advisor: Dr. David Hatchett  
Committee Members:  
Dr. Spencer Steinberg  
Dr. Dong Chan Lee  
Dr. Jacimaria Batista